

1 **The Antimicrobial Peptide Human Beta-Defensin 2 Inhibits Biofilm**  
2 **Production of *Pseudomonas aeruginosa* without Compromising**  
3 **Metabolic Activity**

4 **Kevin R. Parducho<sup>1,2</sup>, Brent Beadell<sup>1</sup>, Tiffany Ybarra<sup>1</sup>, Mabel Bush<sup>1</sup>, Erick Escalera<sup>1</sup>, Aldo T.**  
5 **Trejos, Andy Chieng<sup>2</sup>, Marlon Mendez<sup>1</sup>, Chance Anderson<sup>1</sup>, Hyunsook Park<sup>1</sup>, Yixian Wang<sup>2</sup>,**  
6 **Wuyuan Lu<sup>3</sup>, and Edith Porter<sup>1,\*</sup>**

7 <sup>1</sup>Department of Biological Sciences and <sup>2</sup>Department of Chemistry and Biochemistry, California  
8 State University Los Angeles, Los Angeles, CA, USA

9 <sup>3</sup>Institute of Human Virology and Department of Biochemistry and Molecular Biology, University of  
10 Maryland School of Medicine, Baltimore, MD, USA

11

12 **\* Correspondence:**  
13 Corresponding Author  
14 [eporter@calstatela.edu](mailto:eporter@calstatela.edu)

15

16 **Keywords: Airways, antimicrobial peptides, biofilm, cystic fibrosis, epithelial cells, innate**  
17 **immunity, mucosa, *Pseudomonas aeruginosa***

18

19 **Abstract**

20 Biofilm production is a key virulence factor that facilitates bacterial colonization on host surfaces and  
21 is regulated by complex pathways, including quorum sensing, that also control pigment production,  
22 among others. To limit colonization, epithelial cells, as part of the first line of defense, utilize a  
23 variety of antimicrobial peptides including defensins. Pore formation is the best investigated  
24 mechanism for the bactericidal activity of antimicrobial peptides. Considering the induction of  
25 human beta-defensin 2 (HBD2) secretion to the epithelial surface in response to bacteria and the  
26 importance of biofilm in microbial infection, we hypothesized that HBD2 has biofilm inhibitory  
27 activity. We assessed the viability and biofilm formation of a pyorubin-producing *Pseudomonas*  
28 *aeruginosa* strain in the presence and absence of HBD2 in comparison to the highly bactericidal  
29 HBD3. At nanomolar concentrations, HBD2 – independent of its chiral state – significantly reduced  
30 biofilm formation but not metabolic activity, unlike HBD3, which reduced biofilm and metabolic  
31 activity to the same degree. A similar discrepancy between biofilm inhibition and maintenance of  
32 metabolic activity was also observed in HBD2 treated *Acinetobacter baumannii*, another Gram-  
33 negative bacterium. There was no evidence for HBD2 interference with the regulation of biofilm  
34 production. The expression of biofilm-related genes and the extracellular accumulation of pyorubin  
35 pigment, another quorum sensing controlled product, did not differ significantly between HBD2  
36 treated and control bacteria, and *in silico* modeling did not support direct binding of HBD2 to  
37 quorum sensing molecules. However, alterations in the outer membrane protein profile accompanied  
38 by surface topology changes, documented by atomic force microscopy, was observed after HBD2

39 treatment. This suggests that HBD2 induces structural changes that interfere with the transport of  
40 biofilm precursors into the extracellular space. Taken together, these data support a novel mechanism  
41 of biofilm inhibition by nanomolar concentrations of HBD2 that is independent of biofilm regulatory  
42 pathways.

## 43 Introduction

44

45 Biofilms are composed of microbial communities encased in a protective layer of self-produced,  
46 extracellular polymers. Biofilms are formed on both abiotic and biotic surfaces and play a significant  
47 role in a variety of settings such as aquaculture [1], the food industry, and the clinical field as a factor  
48 for antimicrobial drug resistance. Biofilms can colonize body surfaces and mechanisms regarding  
49 how our bodies prevent biofilm formation are under extensive investigation [2]. In part, biofilms  
50 provide tolerance to host immune factors and antibiotics through impeding their diffusion.  
51 Furthermore, biofilms enhance bacterial resistance to these factors by altering bacterial metabolism  
52 resulting from to the decreased oxygen levels in the center of the biofilm mass as well as the  
53 acidification of the local microenvironment [2; 3; 4; 5]. The biofilm matrix is primarily composed of  
54 exopolysaccharide, proteins, and extracellular DNA and has been particularly well studied in  
55 *Pseudomonas aeruginosa*, a ubiquitous, opportunistic, Gram-negative bacterium. The major  
56 structural polysaccharides of *P. aeruginosa* biofilms are Pel, which is composed of positively  
57 charged amino sugars, and Psl, which is a polymer of glucose, rhamnose, and mannose; and in  
58 certain strains, alginate – an anionic polysaccharide [6; 7; 8]. Proteinaceous components of biofilm  
59 include type 4 pili and cup fimbriae serving attachment and various proteins that connect matrix  
60 components adding strength to the biofilm [9]. Extracellular DNA (eDNA), which is released via cell  
61 lysis [10], plays an important role in priming surfaces for the initial adhesion of the bacteria as well  
62 as in maintaining the structural integrity of the polysaccharide fibers [3; 6; 11; 12; 13; 14].  
63 Multiple regulatory networks govern the complex process of biofilm formation [15], which  
64 progresses from initial attachment mediated by the flagella and the production of pili, to  
65 downregulation of flagellar genes, upregulation of the production and secretion of matrix  
66 components, maturation, and eventual reappearance of flagella and dispersion. For *P. aeruginosa*,  
67 biofilm regulation has been well studied and several regulatory systems have been identified  
68 including the Las, Rhl, and quinolone quorum sensing systems, the GacA/GacS two-component  
69 system, and c-di-GMP controlled pathways. Key quorum sensing molecules for Las, Rhl, and  
70 quinolone systems are N-(3-oxododecanoyl)-homoserine lactone (3-oxo-C12-HSL), N-butanoyl-  
71 homoserine lactone (C4-HSL), and 2-heptyl-3-hydroxy-4-quinolone (known as Pseudomonas  
72 Quorum Sensing molecule or PQS), respectively [16; 17]. These overlapping regulatory systems not  
73 only control the production of biofilm but also the production of pigment and various other virulence  
74 factors [17; 18]. Genes whose expression is modulated during biofilm formation include *flgF*, which  
75 encodes for the basal rod in bacterial flagellin, and *pslA*, which is the first gene in the polysaccharide  
76 synthesis locus [19; 20].

77 In addition to being able to produce biofilm, *P. aeruginosa* possesses potent virulence factors such  
78 as: a type III secretion system, which allows it to directly deliver exotoxins to host cells [21];  
79 rhamnolipids, which enable *P. aeruginosa* to disrupt the tight junctions of respiratory epithelia [22];  
80 and pigments with diverse functions in metal-chelation, competitive inhibition of other bacteria, and  
81 resistance to oxidative stress [23; 24; 25]. All of these virulence factors and resistance mechanisms  
82 contribute to *P. aeruginosa* being one of the leading isolates in healthcare-associated pneumonia in  
83 intensive care units and chronic lung infection in patients with cystic fibrosis, a genetic disorder  
84 characterized by impaired anion transport and increased mucous viscosity [26]. Yet, despite its

85 ubiquity in nature and its prevalence in healthcare-associated infections, *P. aeruginosa* is not known  
86 to cause lung infection in healthy adults, suggesting that humans possess effective innate defense  
87 mechanisms in the airways against this organism.

88 Antimicrobial peptides (AMPs) are small, highly conserved effector molecules that play a key role in  
89 innate immunity [27; 28]. Present in plants, insects, and mammals, most AMPs are between 2 – 5  
90 kDa in size and are cationic with varying degrees of hydrophobicity. Upon the detection of microbial  
91 components via pattern recognition receptors, AMPs can be synthesized by epithelial cells and  
92 myeloid cells as part of the first line of defense against microbes [29; 30; 31; 32; 33]. A wealth of  
93 research has been performed on the ability of AMPs to displace cations bound to bacterial  
94 membranes, which are rich in either negatively charged lipopolysaccharides or lipoteichoic acids in  
95 addition to anionic phospholipids [34]. After binding to bacterial membranes, AMPs can perturb the  
96 membrane structure and form pores mediated by hydrophobic and electrostatic forces. In addition to  
97 the charge of the membrane, phospholipid species and the presence or absence of cholesterol, which  
98 is absent in bacterial membranes, also affect the binding and orientation of AMPs and hence, their  
99 pore-forming capabilities [35; 36; 37; 38; 39; 40]. While pore-formation has been a widely studied  
100 mechanism of action, an increasing body of research suggests that the antimicrobial activity of AMPs  
101 may also depend on other mechanisms – disruption of cell wall synthesis, metabolic activity, ATP  
102 and nucleic acid synthesis, and amino acid uptake [33; 41]. Furthermore, certain AMPs interact with  
103 the eukaryotic host cells and have immunoregulatory functions in addition to their antimicrobial  
104 activity. A notable example is that LL-37 can also: act as a chemotactic agent to recruit other immune  
105 cells and modulate cytokine and chemokine expression in host cells, bind bacterial  
106 lipopolysaccharide, and dysregulate the expression of genes involved in biofilm formation [42; 43;  
107 44; 45; 46]. Other AMPs have also shown multi-functional capabilities, in particular human beta-  
108 defensin 2 (HBD2) and 3 (HBD3), which have been proven to possess mechanisms of action that are  
109 more complex than simple pore formation and membrane perturbation [47; 48; 49]. In fact, HBD2  
110 was the first human beta defensin to demonstrate chemotactic activity [50]. Beta-defensins are  
111 characterized by three, antiparallel  $\beta$ -strands stabilized by three conserved disulfide linkages  
112 preceded by an  $\alpha$ -helical domain near the N-terminus [51; 52; 53]. Although HBD2 and HBD3 share  
113 amino acid sequence and some structural similarities, their overall net charge, hydrophobicity, and  
114 charge distribution differ significantly (**Table 1**) and may play a role in their unique and distinct  
115 mechanisms of action. Expression of HBD2 and HBD3 is low or absent during steady state but both  
116 peptides are induced in airway epithelial tissues during infection or inflammation [31; 32; 48; 54].

117 Due to their lasting potency for millions of years and the feasibility of modifying AMP structures,  
118 AMPs continue to be in the spotlight as potential antimicrobial agents [33]. The importance of  
119 biofilm in the infection process and in their resistance to antimicrobial agents has been recognized,  
120 yet there is a lack of drugs that interfere with biofilm. Therefore, knowledge on the structure-function  
121 relationships of AMPs, and the effects of AMPs on bacterial biofilm formation may benefit rational  
122 engineering and design of novel AMP variants and therapeutic regimens that are effective against  
123 microbial biofilms [55]. Considering the induction of HBD2 and HBD3 and their secretion to the  
124 epithelial surface in response to bacteria and their products, we hypothesized that HBD2 and HBD3  
125 have biofilm inhibitory activity. We discovered that biofilm and metabolic inhibition are  
126 proportionally reduced by HBD3 but not by HBD2. At low concentrations, HBD2 inhibits biofilm  
127 production, but not metabolic activity. We undertook multiple approaches to delineate the underlying  
128 mechanism for the selective biofilm inhibitory effects of HBD2. This research may lead to the  
129 identification of novel targets for the engineering of antimicrobials, which, in the era of increasing  
130 multi-drug resistance, is of great importance.

131

## 132 **Materials and Methods**

133

### 134 **Antimicrobial peptides**

135 Chemical synthesis and purification of human beta-defensin 2 (HBD2/L-HBD2), its D- form (D-  
136 HBD2) comprised entirely of D-amino acids, its linearized mutant (Linear HBD2 with alanine  
137 replacing all cysteine residues), and human beta-defensin 3 (HBD3, in L-form) have been described  
138 previously [56; 57]. **Table 1** summarizes their physicochemical properties. Stock solutions (500  $\mu$ M)  
139 were prepared in 0.01% acetic acid and stored at  $-20$  °C. For experiments, peptides were used as 10-  
140 fold concentration in 0.01% acetic acid.

141

### 142 **Bacterial culture**

143 For this study, a pyorubin-producing *P. aeruginosa* strain (a cystic fibrosis isolate previously  
144 obtained from Dr. Michael J. Welsh, University of Iowa, Iowa City) and *A. baumannii* ATCC 19606  
145 were used. For each experiment, snap-frozen 18 h cultures in Tryptic Soy Broth (TSB) (Oxoid) were  
146 quickly thawed, subcultured into prewarmed TSB (750  $\mu$ L into 50 mL), and brought to mid-log  
147 growth phase (3 h at 37 °C, 200 rpm). Bacterial cells were then sedimented and washed with 140 mM  
148 NaCl by centrifugation for 10 min at  $805 \times g$  in a precooled centrifuge (4 °C), and resuspended in  
149 500  $\mu$ L 140 mM NaCl. For gene expression analysis, the suspended bacteria were used directly. For  
150 all other assays, the concentration of bacteria was first adjusted to  $5 \times 10^7$  CFU/mL in 140 mM NaCl,  
151 and then further diluted as needed.

152

### 153 **Biofilm quantification**

154 In a round bottom 96-well polystyrene microtiter plate (Costar #3795), 90  $\mu$ L mid-logarithmic  
155 growth phase bacteria were added to 10  $\mu$ L of 10-fold concentrated defensin or 0.01% acetic acid as  
156 solvent control to yield the following final assay conditions:  $1 \times 10^6$  CFU/mL, 10% Mueller-Hinton  
157 broth (Oxoid, without cations), and 140 mM NaCl. Samples were incubated for 18 h at 37 °C and  
158 biofilms were quantified according to Merritt *et al.* [58]. Briefly, the content of sample wells  
159 containing non-adherent bacteria (planktonic and/or dead) was carefully discarded without disturbing  
160 the biofilm, and the well walls were rinsed three times with dH<sub>2</sub>O (200  $\mu$ L/well) followed by addition  
161 of 125  $\mu$ L of 0.1% crystal violet (Sigma-Aldrich, St. Louis, MO). After 10 min incubation at RT, the  
162 crystal violet solution was removed, wells were rinsed three times with dH<sub>2</sub>O (200  $\mu$ L/well) and air  
163 dried for at least 30 min. To solubilize crystal violet bound to biofilm, 200  $\mu$ L of 30 % acetic acid  
164 was added to each well and after 15 min incubation at RT 125  $\mu$ L was transferred to optically clear  
165 flat-bottom 96-well polystyrene microtiter plates (Perkin Elmer from Waltham, MA USA).  
166 Absorbance was read at 570 nm using a Victor X3 Plate Reader (Perkin Elmer). Wells containing  
167 only 125  $\mu$ L of 30 % acetic acid were used to subtract baseline absorbance values from samples for  
168 analysis.

169

### 170 **Metabolic activity measurement**

171 Resazurin reduction was employed as a measure of bacterial metabolic activity [59; 60]. Metabolites  
172 accumulating during bacterial growth reduce the weakly fluorescent resazurin to the highly  
173 fluorescent resorufin. Samples were prepared as described above but with resazurin (Sigma) added to  
174 the assay buffer to obtain a final concentration of 0.01% resazurin (w/v). Relative fluorescent units  
175 (RFU) were measured every 3 h with a preheated Victor X3 Plate Reader (Perkin Elmer) at 530 nm  
176 excitation and 616 nm emission wavelength and a top read.

177

178

179

### 180 **ATP quantification**

181 ATP concentrations of non-adherent bacteria were determined using the BacTiterGlo kit (Promega),  
 182 with ATP standard curves prepared according to the manufacturer's instructions. Bacteria were  
 183 prepared and incubated with defensins for 18 h as described for the biofilm assay. Then, the entire  
 184 well contents were transferred to a new 96 well plate, thoroughly resuspended, and of this 75  $\mu$ L  
 185 from each well was transferred to a black 96-well half area plate (Perkin-Elmer). After addition of  
 186 75  $\mu$ L ATP substrate solution to each well and 5 min mixing on an orbital shaker, luminescence was  
 187 quantified with a Victor X3 plate reader. Seventy-five  $\mu$ L aliquots of serially diluted ATP standard  
 188 were treated in the same way.

### 190 **Pyorubin quantification**

191 Pyorubin is a collection of pigments produced by certain *P. aeruginosa* strains including our test  
 192 strain. Although its full chemical composition is unknown, it consists of at least two, water-soluble,  
 193 red-colored pigments [61]. Pyorubin quantification was based on Hosseinidou *et al.* [23]. Briefly,  
 194 bacteria were grown for 18 h in 10% Mueller-Hinton and 140 mM NaCl in the presence of 0.125 to 1  
 195  $\mu$ M of HBD2 or solvent control in final assay volumes of 1 mL in 12-well microtiter plate (non-tissue  
 196 culture treated, Costar). After 18 h incubation, well contents were collected and centrifuged at 5,000  
 197  $\times g$  for 10 min at 4  $^{\circ}$ C to remove non-adherent bacteria. Equivolume mixtures of cell free supernatant  
 198 (900  $\mu$ L) and chloroform (900  $\mu$ L) were mixed and centrifuged at 12,000  $\times g$  for 15 min at 4  $^{\circ}$ C to  
 199 separate the aqueous and organic phases and remove cell debris and other molecules. The aqueous  
 200 phase containing pyorubin was lyophilized, dissolved in 125  $\mu$ L volume of dH<sub>2</sub>O. From this, 100  
 201  $\mu$ L were transferred to a 96-well flat bottom plate (Perkin Elmer) followed by an absorbance reading  
 202 at 535 nm using a Victor X3 Plate Reader (Perkin Elmer).

### 205 ***In silico* molecular docking studies**

206 The *in silico* modeling of binding between QS molecules and HBD2 was performed using Autodock  
 207 Vina (The Scripps Research Institute) through the UCSF Chimera program  
 208 (<https://www.cgl.ucsf.edu/chimera/>). LasR receptor (RSCB 3IX3) and HBD2 (RSCB 1FQQ) were  
 209 considered as rigid receptors and were docked with *N*-(3-oxododecanoyl) homoserine lactone (3-oxo-  
 210 C12-HSL), *N*-butanoyl homoserine lactone (C4-HSL), and 2-heptyl-3-hydroxy-4-quinolone (PQS) as  
 211 ligands. Phosphorylcolamine (NEtP) was used as a negative control. Free energy of binding was used  
 212 to calculate dissociation constants using equation (1) with  $R = 0.00198$  kcal/(mol K) and  $T = 37$   $^{\circ}$ C =  
 213 310.15 K [62].

$$214 K_{D,pred} = e^{([\Delta G_{bind}]/[(R/1000)*T])} \quad (1)$$

### 216 **Gene expression analysis**

217 Mid-logarithmic growth phase bacteria were prepared and washed as described above. The assay was  
 218 up-scaled using 12-well polystyrene flat bottom plates with non-reversible lids with condensation  
 219 rings (Genesee Scientific, San Diego, CA, USA). Twenty  $\mu$ L of the washed bacteria was added to  
 220 HBD2 or solvent (100  $\mu$ L of 10-fold concentrated defensin in 0.01% acetic acid or 0.01% acetic  
 221 acid, respectively, diluted in 900  $\mu$ L 10% Mueller Hinton/140 mM NaCl) yielding about  $1 \times 10^8$   
 222 CFU/mL. After incubation at 37  $^{\circ}$ C for the specified time points, biofilm and planktonic phase  
 223 bacteria were homogenized by 10 min vortexing with 1 mm glass beads and tightly secured lids  
 224 (Sigma-Aldrich, St. Louis, MO, USA). RNA extraction was performed on the homogenized samples  
 225 using an RNeasy Mini Kit (Qiagen, Hilden, Germany) following the manufacturer's enzymatic lysis  
 226 and mechanical disruption protocol with acid-washed 425-600  $\mu$ m glass beads (Sigma-Aldrich).  
 227 Residual genomic DNA was removed with in-solution TurboDNase treatment (2 U/ $\mu$ L, Invitrogen,

228 Carlsbad, CA, USA) according to the manufacturer's recommendations followed by purification and  
229 concentration of RNA samples with RNA Clean & Concentrator-5 kit (Zymo Research, Irvin, CA,  
230 USA). Purity of RNA was confirmed by lack of amplification in SsoAdvanced™ Universal SYBR®  
231 Green (Bio-Rad, Hercules, CA, USA) real-time PCR using the RNA samples as template and primers  
232 for the housekeeping gene *gapA* (see **Table 2**). Confirmed pure RNA samples were reverse  
233 transcribed with iScript Reverse Transcription Supermix (Bio-Rad) and resulting cDNA was diluted  
234 to 25 ng/μL in nuclease free water. SsoAdvanced™ Universal SYBR® Green real-time PCR was  
235 performed with target primers for *pslA* and *flgF* and housekeeping gene *gapA* as reference gene (see  
236 **Table 2**, used at 0.75 μM final concentrations) in 10 μL reaction volumes and 12.5 ng cDNA input.  
237 Primers (Integrated DNA Technology's, IDT, Coralville, IA, USA) were designed using IDT's  
238 primerQuest Tool. Quantitative PCR (qPCR) and subsequent melt curve was performed using BIO-  
239 RAD's CFX96 Real Time Thermocycler following standard conditions with annealing/extension at  
240 60°C. CT values and relative gene expression were determined with BIO-RAD's CFX Maestro  
241 Version 1.1. Amplified products were verified through size determination via standard agarose gel  
242 electrophoresis and melt curve analysis. Each time point was assessed in three independent  
243 experiments conducted in duplicates for a total n of 6. Initially, *16S rRNA* was considered as a second  
244 housekeeping gene. However, its CT values (around 5) were substantially earlier than the CT values  
245 for the target genes and *gapA* (at or above 20) and thus, *16S rRNA* gene expression was not further  
246 evaluated in this study.

247

### 248 **Outer membrane protein profile analysis**

249 *P. aeruginosa* outer membranes were harvested after incubation with HBD2 or solvent control  
250 according to Park et al. 2015 [63] with minor modifications. Briefly, bacteria were prepared as above  
251 and then grown for 18 h in 10% Mueller-Hinton and 140 mM NaCl in the presence of 0.125 to 1 μM  
252 of HBD2 or solvent control in final assay volumes of 1 mL in 12-well microtiter plate (Costar® not  
253 treated, Corning). After 18 h incubation, the well contents were resuspended, transferred into  
254 microfuge tubes, and centrifuged at 5,000 × g for 10 min at 4 °C to pellet the bacterial cells. Cells  
255 were then resuspended in 80 μL of 0.2 M Tris-HCl, pH 8.0. Then, 120 μL lysis buffer was added to  
256 the resuspended cells (final conditions were 200 μg/mL hen egg white lysozyme (Sigma-Aldrich), 20  
257 mM sucrose and 0.2 mM EDTA in 0.2 M Tris-HCl, pH 8.0). After a 10 min incubation at RT, 2 μL  
258 of Protease Inhibitor Cocktail (Sigma Aldrich P8340) was added followed by 202 μL of extraction  
259 buffer (10 μg/mL DNase I [Sigma-Aldrich DN25] in 50 mM Tris-HCl/10 mM MgCl<sub>2</sub>/ 2 % Triton  
260 X-100). After 1.5 h incubation on a rocker at 4°C, samples were centrifuged at 1500 × g at 4°C for 5  
261 min. The resulting supernatants from triplicate samples, which contain the outer membranes, were  
262 pooled and placed into 4 mL ultrafiltration tubes with 5 kDa cut off molecular weight (Amicon  
263 Ultracel, 5k, Millipore). PBS was added to yield a volume of 4 mL, and then the tubes were  
264 centrifuged at 2400 ×g until about 500 μL residual volume was obtained. The outer membranes in  
265 this residual were then washed by suspending in 3.5 mL PBS and then centrifuging at 2400 ×g for 25  
266 min at RT, yielding a residual volume of approximately 200 μL. Of this, 4 μL were subjected to  
267 standard SDS-PAGE using Bio-Rad 16.5 % Mini-Protean Tris-Tricine gels followed by silver stain.  
268 Images were acquired with Versadoc (Bio-Rad) and analyzed with Image Lab version 6.01 software  
269 from Bio-Rad Laboratories.

270

### 271 **Atomic force microscopy**

272 *P. aeruginosa* (1 × 10<sup>6</sup> CFU/mL inoculum) was incubated in 10 % Mueller Hinton broth/140 mM  
273 NaCl/12.5 mM sodium phosphate pH 7.0 with and without HBD2 (0.25 μM), on glass coverslips  
274 (Borosilicate glass square coverslips, Fisher Scientific) in 6-well plates (Corning) for 18 h at 37°C.  
275 As negative controls for HBD2 the peptide solvent 0.01% acetic acid was included, respectively.

276 Coverslips were then transferred into wells of a fresh 6-well plate and adherent bacteria were fixed  
277 with 2.5 % glutaraldehyde (Ted Pella, CA; 0.25% in PBS, electron microscopy grade) for 20 min at 4  
278 °C followed by washing with deionized water according to Chao and Zhang, 2011 [64], and stored at  
279 4°C until imaging by atomic force microscopy (AFM).

280 All AFM tests [65] were carried out with a NX12 AFM system (Park System) using an aluminum  
281 coated PPP NCHR (Park systems) cantilever with a spring constant of 42 N/m, a resonance  
282 frequency of 330 kHz, and a nominal tip radius of < 10 nm. At least five images were acquired per  
283 sample in air with non-contact mode (NCM) with settings of 256 pixels/line and 0.75 Hz scan rate  
284 and continuous monitoring of the tip integrity. The images were first order flattened and the  
285 roughness and height of all bacteria were measured using XEI software (Park Systems). Specifically,  
286 roughness of each bacterium was calculated from the root mean square value (RMS, i.e. standard  
287 deviation of the distribution of height over the whole bacterium surface).

288  
289

### 290 **Data and statistical analysis**

291 Data graphs were generated using Microsoft Excel® 2016 or Graphpad Prism 7.04 Software.  
292 Statistical analyses were performed using IBM SPSS version 24 or Graphpad Prism 7.04 Software. A  
293 p-value < 0.05 was considered statistically significant.

294  
295

### 296 **Results**

297

#### 298 **At low concentrations, HBD2 does not reduce metabolic activity but inhibits biofilm production** 299 **by *P. aeruginosa*, unlike HBD3**

300 To compare the antimicrobial activities of HBD2 and HBD3, *P. aeruginosa* was exposed to either  
301 peptide at various concentrations over a period of 18 h. Viability was assessed by measuring  
302 metabolic activity every 3 h via quantification of resazurin reduction to the highly fluorescent  
303 resorufin by bacterial metabolites. Biofilm was assessed at 18 h post-incubation via quantification of  
304 crystal violet staining through absorbance readings. The resazurin reduction assay showed that both  
305 HBD2 and HBD3 reduced metabolic activity in a dose-dependent manner, with HBD3 being more  
306 effective on a per molar basis, producing around a 30% reduction at 0.5 µM compared to the 4 µM  
307 needed by HBD2 at 18 h for the same effect (**Figure 1**). However, when comparing the effect on  
308 biofilm production between the two peptides, a notable difference was observed. At concentrations of  
309 0.25 and 0.5 µM, HBD2 reduced *P. aeruginosa* biofilm to ~ 75% of the control without significantly  
310 reducing the metabolic activity (**Figure 2A**). In contrast, at these concentrations, HBD3 reduced the  
311 formation of *P. aeruginosa* biofilm in a dose dependent manner that was directly proportional to the  
312 cumulative effect on metabolic activity and further reduced both biofilm and resorufin production to  
313 nearly undetectable levels at a concentration of 1 µM (**Figure 2B**) consistent with direct microbicidal  
314 activity. ATP concentrations measured at the end of the 18 h incubation period corroborated the  
315 resazurin data (**Figure 3**), showing maintained ATP levels in HBD2 treated bacteria but a significant  
316 reduction of ATP levels in HBD3 treated *P. aeruginosa* (at 2 µM defensin, 17.65 ± 5.31 nM ATP  
317 compared to 3.6 ± 2.88 nM ATP, respectively,  $p = 0.011$ ). These data suggest a differential  
318 mechanism for the antimicrobial activity between HBD2 and HBD3, and that HBD2 selectively  
319 inhibits biofilm formation at low concentrations.

320  
321

#### 322 **HBD2 similarly inhibits biofilm production by *A. baumannii* without reducing metabolic** 323 **activity at lower concentrations**

324 To rule out that the observed differential biofilm reducing activity of HBD2 activity was strain-  
325 specific and restricted to *P. aeruginosa*, we also subjected *A. baumannii*-another opportunistic Gram-  
326 negative rod of clinical relevance - to varying doses of HBD2 and determined resazurin reduction and  
327 biofilm production after 18 h incubation. As shown in **Figure 4**, at low concentrations, HBD2  
328 similarly inhibited biofilm formation while not reducing metabolic activity of *A. baumannii*. For  
329 example, at 1  $\mu\text{M}$ , HBD2 effected a significant reduction of biofilm to  $51.77 \pm 2.93$  % of the control  
330 ( $p < 0.001$ ) while resazurin reduction was still at  $115 \pm 0.67$  % ( $p = 1.0$ .) of the control (means  $\pm$  S.D,  
331  $n = 3$ ). At higher concentrations though, HBD2 appeared to have greater effects on *A. baumannii*  
332 compared to *P. aeruginosa* as both biofilm and metabolic activity were reduced to less than 2 % and  
333 20 % of the control at 4  $\mu\text{M}$  HBD2, respectively ( $1.23 \pm 0.48$  % and  $18.71 \pm 10.43$  %, means  $\pm$  S.D,  
334  $n = 3$ ).

### 336 **HBD2 biofilm inhibitory activity does not depend on chirality but on folding state**

337 Since HBD2 appeared to selectively reduce biofilm formation and it has been known to bind to  
338 chemokine receptors on eukaryotic cells [66; 67], it was possible that the effects of HBD2 were due  
339 to binding to receptors involved in the biofilm regulatory pathway such as the GacA/GacS system.  
340 To test this, we assessed the activity of the D-form of HBD2, which, due to mismatched chirality,  
341 does not bind to proteinaceous receptors of L-HBD2. Like L-HBD2, D-HBD2 effected a significant  
342 reduction of biofilm production by *P. aeruginosa* without reducing metabolic activity (**Figure 5A**).  
343 Thus, this suggests that the observed HBD2 effect on *P. aeruginosa* biofilm production was not due  
344 to binding to receptors important for biofilm regulatory pathways.

345 Upon proper folding, defensins form three intramolecular disulfide bridges, which stabilize an  
346 amphipathic structure where cationic and hydrophobic amino acid residues are spatially segregated.  
347 To assess the importance of the structure and thus, charge distribution of HBD2 for its observed  
348 activity, a comparison was made between wildtype HBD2 and a linearized HBD2 mutant (Linear  
349 HBD2) with cysteine residues replaced by alanine residues. Loss of the cysteine residues prevents the  
350 formation of stabilizing disulfide bonds, drastically limits proper folding, and disrupts the  
351 organization of charged domains thought to be critical for AMP activity [68; 69; 70]. As shown in  
352 **Figure 5B**, linearization of HBD2 resulted in a pronounced loss of activity.

353 Taken together, these data provided evidence for a receptor-independent activity that requires proper  
354 sequestration of charged and hydrophobic residues. We next asked whether HBD2 disrupts  
355 regulatory pathways of biofilm production through QS molecule binding. To answer this question,  
356 we took a three-pronged approach and performed *in silico* docking studies with known QS molecules  
357 involved in biofilm regulation, employed qPCR probing for genes differentially expressed during  
358 biofilm formation, and quantified pyorubin, a pigment regulated by the pathways that also affect  
359 biofilm production.

### 361 **HBD2 binding to QS molecules is unlikely based on Autodock Vina prediction**

362 QS molecules are small and flexible molecules with a potential for hydrogen bonding and  
363 hydrophobic interactions. Thus, they may bind to and be sequestered by HBD2. To explore this  
364 further, Autodock Vina was used (**Figure 6**) to predict HBD2 binding to known *P. aeruginosa* QS  
365 molecules representing three different QS systems, namely 3-oxo-C12-HSL – as the major QS  
366 molecule for *P. aeruginosa* utilized by the Las system, C4-HSL primarily utilized by the Rhl  
367 system, and PQS a key sensing molecule in the 4-quinolone system [71]. As a positive control,  
368 Autodock Vina was also used to match the known binding pocket of the QS molecule 3-oxo-C12-  
369 HSL to its receptor LasR that has been previously assessed by X-ray diffraction (RSCB 3IX3 [72]).  
370 Phosphorylcolamine (NEtP), which is not expected to bind to either LasR receptor or HBD2, was  
371 used as a negative control. Using the same methodology that confirmed binding of 3-oxo-C12-HSL



372 to LasR here, (**Figure 6A**) no binding of 3-oxo-C12-HSL to HBD2 was found (**Figure 6B**).  
373 Furthermore, we calculated the free energy of binding and found for LasR values corresponding to  
374 those reported in the literature [62; 73]. Employing a -6 kcal/mol threshold for likely binding  
375 between ligand and receptor, binding between LasR and 3-oxo-C12-HSL, C4-HSL, and PQS was  
376 much more favorable (**Figure 6C**) than binding between HBD2 and these sensing molecules (**Figure**  
377 **6D**).

378 Using equation [1], the dissociation constants ( $K_D$ ) for the most favorable binding pair between either  
379 LasR or HBD2 with each QS molecule was calculated (**Table 3**). This method predicted the  $K_D$  of 3-  
380 oxo-C12-HSL and LasR (1.15  $\mu\text{M}$ ) near that of previously reported values ( $\sim 5.5 \mu\text{M}$ ) [74].  
381 Furthermore,  $K_D$  values for LasR binding with all three *P. aeruginosa* QS molecules were  
382 consistently two to three orders of magnitude lower than those of HBD2 binding with any of these  
383 QS molecules. This suggests that it is unlikely for HBD2 at physiological concentrations [75; 76; 77]  
384 to significantly bind these QS molecules.

385

### 386 **Gene expression of *flgF* and *pslA* is not affected by HBD2**

387 During biofilm formation, motility and production of exopolysaccharide are reciprocally regulated  
388 with reduction of the expression of flagella-related genes and increase in the expression of genes  
389 contributing to polysaccharide synthesis including PIs polysaccharide. Thus, we compared the  
390 expression of *flgF* (**Figure 7A**) and *pslA* (**Figure 7B**) in *P. aeruginosa* treated with 0.25  $\mu\text{M}$  HBD2  
391 or solvent at various timepoints for up to 12 h. For solvent treated control bacteria, as expected, *flgF*  
392 gene expression decreased within 2 h reaching statistical significance after 6 h and the expression of  
393 *pslA* was significantly increased after 2 h compared to the later time points ( $p < 0.01$  and  $p < 0.05$  in  
394 multivariate ANOVA with Bonferroni posthoc analysis). As observed for control bacteria, *flgF* gene  
395 expression decreased over time and was significantly reduced in HBD2 treated bacteria ( $p < 0.05$ )  
396 though changes in *pslA* gene expression did not reach statistical significance. However, there was  
397 overall no statistical significant difference between solvent and HBD2 treated bacteria. Thus,  
398 expression analysis of genes altered early in the biofilm production process does not support that  
399 HBD2 interference with biofilm production occurs at the transcriptional level.

400

### 401 **Pyorubin accumulation is not reduced in media collected from HBD2 treated *P. aeruginosa***

402 Pigment production in *P. aeruginosa* has been shown to be also regulated by QS [24; 61]. To further  
403 corroborate that HBD2 does not interfere with QS, we quantified pyorubin released into culture  
404 supernatants in the presence and absence of HBD2. At 0.125 and 0.25  $\mu\text{M}$  HBD2 there was no  
405 difference in pyorubin accumulation compared to the control (data not shown). In the presence of 0.5  
406 and 1  $\mu\text{M}$  HBD2, there was a slight increase of pyorubin ( $109.5 \pm 4.9\%$  and  $109.9 \pm 5.8\%$  of the  
407 control, respectively,  $p < 0.01$  in univariate ANOVA with Bonferroni posthoc adjustment). This  
408 finding further supports that HBD2 does not inhibit quorum sensing and next, we explored whether  
409 HBD2 may induce structural changes in the outer membrane that could interfere with the transport of  
410 biofilm precursors to the extracellular space.

411

412

### 413 **HBD2 alters the outer membrane protein profile of *P. aeruginosa***

414 Outer membrane proteins participate in the process of biofilm formation [78]. Hence, we probed  
415 whether incubation with HBD2 leads to changes in the outer membrane protein profile of *P.*  
416 *aeruginosa* (**Figure 8**). A representative image of outer membrane preparations resolved by silver  
417 stained SDS-PAGE is depicted in **Figure 8A**. Numerous bands are detected ranging from about 10  
418 kDa to over 200 kDa with the most dominant bands appearing above 25 kDa, in particular a band  
419 around 35 kDa similar to the molecular weights of previously reported *P. aeruginosa* outer

420 membrane proteins [79]. Two weaker bands around 10 kDa are consistently visible only in the outer  
421 membrane preparations from control bacteria. Overall, the outer membranes from HBD2 treated  
422 bacteria appear to contain less proteins between 35 and 75kDa. A prominent band between 10 and 15  
423 kDa is detected in all samples, including the medium control, consistent with the molecular weight of  
424 the lysozyme (14 kDa) added during the extraction procedure. **Figure 8B** summarizes the protein  
425 profiles of the outer membrane preparations from control bacteria and HBD2 treated bacteria. To  
426 control for variations during the ultrafiltration process and gel loading, the band intensities of the  
427 various proteins were normalized with the presumptive lysozyme band intensity. HBD2 appears to  
428 affect a decrease in outer membrane proteins in particular at about 22 kDa, 34 kDa, 40 kDa, 45 kDa,  
429 and 50 kDa, with the changes noticeable at all concentrations tested.

430

431

432

### 433 **Atomic force microscopy reveals ultrastructural changes in HBD2 treated bacteria reflected in** 434 **increased surface roughness**

435 We also assessed whether the changes at the outer membrane induced by HBD2 resulted in

436 topographical changes and employed atomic force microscopy to measure bacterial height and

437 roughness after incubation for 18 h in the presence or absence of 0.25  $\mu$ M HBD2 (**Figure 9**).

438 Representative images of control and HBD2 treated bacteria are shown in **Figure 9A**. The surface of

439 control bacteria appears smoother compared to the surface of HBD2 treated bacteria, the latter

440 showing irregular dents. While the overall bacterial height is not significantly different in HBD2-

441 treated bacteria compared to solvent only exposed bacteria ( $215.22 \pm 3.96$  nm *versus*  $220.24 \pm 3.23$

442 nm, means  $\pm$  S.E.M, n = 85 and n = 69, respectively,  $p = 0.343$ ), there is a significant increase in

443 roughness in HBD2 treated samples (**Figure 9B**) consistent with a structurally altered surface ( $43.39$

444  $\pm 1.52$  *versus*  $51.86 \pm 1.5$  nm, means  $\pm$  S.E.M., n = 85 and n = 69,  $p < 0.001$  in independent samples

445 T test).

446

447

448 Taken together, our data demonstrate that at low concentrations L- and D-forms of HBD2 inhibit

449 biofilm formation while not reducing metabolic activity in Gram-negative bacteria of two different

450 genera, *Pseudomonas* and *Acinetobacter*. Furthermore, this activity appears to be receptor-

451 independent and not mediated by interference with quorum sensing or other regulatory pathways of

452 biofilm production at the transcriptional level. Instead, our data are consistent with structural changes

453 induced by HBD2 that interfere with the transport of biofilm precursors into the extracellular space

454 suggesting a novel mechanism of action for the antimicrobial peptide HBD2.

455

456

## 457 **Discussion**

458

459 In this study, we demonstrate that, HBD2, at nanomolar concentrations, and independent of its chiral  
460 state, significantly reduced biofilm formation of *P. aeruginosa* without affecting metabolic activity.

461 This was unlike HBD3, which equally reduced biofilm and metabolic activity at nanomolar

462 concentrations. HBD2 similarly affected *A. baumannii*, another Gram-negative bacterium, at low

463 concentrations. *In silico* modeling did not support direct binding of HBD2 to QS molecules, the

464 release of a QS regulated pigment was not inhibited, and the expression of biofilm-related genes was

465 not influenced by HBD2. However, the outer membrane protein profile was altered in HBD2 treated

466 bacteria with reduced representation of several proteins, which was accompanied by increased

467 roughness of the bacterial surface. Taken together, these data support a novel mechanism of biofilm

468 inhibition by HBD2 at low concentrations that is independent of biofilm regulatory pathways but

469 involves structural changes induced by HBD2 that may interfere with the transport of biofilm  
470 precursors into the extracellular space.

471  
472 HBD2 has been previously reported to reduce bacterial survival in existing biofilm cultures of  
473 *Lactobacillus ssp.*, Gram-positive bacteria, at higher, micromolar concentrations. [80]. However,  
474 inhibition of biofilm formation by HBD2 has not been reported previously to the best of our  
475 knowledge. Considering the rapid induction of HBD2 in epithelial cells' response to  
476 proinflammatory cytokines and bacterial challenge [81], the ability to interfere with biofilm  
477 formation at low concentrations adds importance to the role of HBD2 in innate host defense during  
478 the early interaction between host and pathogen. Bacteria are more susceptible to host-derived and  
479 exogenous antimicrobial agents while they are metabolically active in the planktonic state prior to  
480 biofilm production. Thus, HBD2 may amplify host defenses early in the attempted infection process  
481 and could improve the action of antibiotics in a clinical setting [82]. Synergism studies will be able to  
482 address this experimentally in the future.

483  
484 Anti-biofilm activity of HBD2 in the absence of inhibition of metabolic activity of *P. aeruginosa*  
485 occurred only at low concentrations. A concentration dependent mechanism of action has been well  
486 documented for the lantibiotic nisin, which, at nanomolar concentrations, preferentially binds to lipid  
487 II disrupting cell wall synthesis and, at micromolar concentrations, embeds into the bacterial  
488 membrane causing pore formation [83; 84; 85; 86; 87]. More recently, the alpha-defensin human  
489 neutrophil peptide 1 (HNP1) has been added to the list of antimicrobial peptides that initially interact  
490 with lipid II, and when concentrations increase, with the bacterial cell membrane [88]. Binding of  
491 HBD3 to lipid II has also been described, albeit at higher concentrations, in the micromolar range  
492 [47]. It is conceivable that HBD2 could similarly interfere with membrane-embedded proteins  
493 responsible for the transport of biofilm components [17] at low concentrations followed by  
494 membrane perturbation at higher concentrations.

495  
496 The differential effect of HBD2 on biofilm production and metabolic activity of *P. aeruginosa* was  
497 not observed in the related beta-defensin HBD3, which was active at lower concentrations than  
498 HBD2 and equally reduced biofilm and metabolic activity reflecting a strong bactericidal activity.  
499 These differences in their activity could be at least in part attributed to the differences in their  
500 physicochemical properties with respect to net charge, surface charge distribution, hydrophobicity  
501 index, and behaviour in solution [51; 89]. Biofilm is a complex matrix with numerous components  
502 that can be affected in different ways by HBD2 and HBD3. For example, alginate has been shown to  
503 affect antimicrobial peptide conformation inducing alpha-helices contingent on the hydrophobicity  
504 [90], and HBD2 and HBD3 substantially differ in their hydrophobicity with HBD2 being more  
505 hydrophobic than HBD3.

506  
507 HBD2, at low concentrations, similarly inhibited biofilm production in *A. baumannii* without  
508 reducing metabolic activity suggesting the observed effects are not strain specific. However, at higher  
509 HBD2 concentrations differences between the effects on *P. aeruginosa* and *A. baumannii* emerged as  
510 reflected in a near complete inhibition of biofilm production of *A. baumannii* contrasting the stalled  
511 biofilm inhibition of *P. aeruginosa*. The lesser susceptibility of *P. aeruginosa* to HBD2 may be due  
512 to a greater outer membrane vesicle production in *P. aeruginosa* that may sequester HBD2 before it  
513 reaches the bacterial cell [91].

514  
515 Like other defensins, HBD2 forms three intramolecular disulfide bridges and linearization of the  
516 peptide can reveal the importance of its structure for its antimicrobial activity [92]. Here,  
517 linearization of full length HBD2 led to a pronounced loss of both its antimicrobial and biofilm

518 inhibitory activity. This contrasts reports for other defensins including HBD3 and could be attributed  
519 to a lack of accumulation of positively charged amino acid residues at the C-terminus of HBD2  
520 compared to HBD3. Chandrababu and colleagues [93] have shown that positively charged residues  
521 cluster in the C-terminal segment of a linearized form of HBD3 allowing them to interact with the  
522 negatively charged phospholipids of micelles. The inherent antimicrobial activity of this patch of  
523 cationic residues is also reflected in studies with HBD3 analogues truncated to the C-terminal region  
524 [94]. The here observed loss of activity after linearization could indicate that HBD2 functions  
525 through a receptor [56]. However, D- and L forms of HBD2 did not differ in their activity and thus,  
526 we interrogated the possibility that HBD2 interferes with regulatory networks of biofilm production.

527  
528 QS molecules are key to the regulation of virulence factor production including biofilm and pigment  
529 in *P. aeruginosa*. They are small hydrophobic molecules [95] and thus, we interrogated possible  
530 binding of HBD2 to QS molecules *in silico*. We found favorable binding of LasR to not only its  
531 cognate ligand 3-oxo-C12-HSL but also to C4-HSL and PQS. This is in line with a recent study  
532 describing LasR as promiscuous for binding a variety of QS molecules [96]. The unfavorable binding  
533 energies derived for HBD2 suggest that interference of QS-dependent processes through direct  
534 HBD2 binding to individual QS molecules is unlikely. Another type of QS molecule, (2S,4S)-2-  
535 methyl-2,3,3,4-tetrahydroxytetrahydrofuran-borate (S-THMF-borate), has been shown to increase  
536 biofilm formation in *P. aeruginosa* [97; 98]. However, although S-THMF-borate – a molecule with a  
537 distinct structure from major Gram-negative QS molecules – has been identified in some Gram-  
538 positive and Gram-negative bacteria [99], *P. aeruginosa* does not encode the *luxS* gene required for  
539 its synthesis [100] and binding to this S-THMF-borate should not be further considered as an  
540 underlying mechanism for the observed biofilm inhibition.

541  
542 In agreement with the *in silico* data, HBD2 did not affect the expression of *flgF* and *pslA*. Thus,  
543 interference of HBD2 with regulatory networks at the transcriptional level is not likely to account for  
544 its biofilm inhibitory activity. However, we cannot rule out that HBD2 has posttranscriptional effects  
545 through interference with the two component signal transduction system GacS/GacA [71; 101]. GacS  
546 is a transmembrane sensor kinase phosphorylating GacA, which in turn induces the expression of  
547 small RNA molecules that antagonize the protein RsmA, a translational repressor interfering with *psl*  
548 translation and known to normally block exopolysaccharide production [102]. It is conceivable that  
549 HBD2 could interfere with GacS upon inserting into the bacterial membrane. Finally, HBD2 might  
550 bind to the secondary messenger molecule c-di-GMP, which regulates biofilm formation in *P.*  
551 *aeruginosa* at multiple levels [103]. Previously, de la Fuente-Nunez and colleagues [104]  
552 demonstrated that peptide 1018, derived from the antimicrobial peptide bovine Bac2a [105], inhibited  
553 biofilm formation in *P. aeruginosa* while not affecting planktonic growth by binding to the second  
554 messenger p(pp)Gpp and promoting its degradation. A similar mode of action could apply to HBD2.

555  
556 Further supporting that HBD2 does not act through interference with regulatory networks is our  
557 finding that pyorubin accumulation in the extracellular fluid was not diminished after incubation with  
558 HBD2. Pyorubin is composed of several pigments including aeruginosin A, which is a phenazine,  
559 like the much better studied *P. aeruginosa* pigment pyocyanin [106]. Phenazines typically traverse  
560 the bacterial membrane freely and their production is under the same controls that govern biofilm  
561 production [107; 108].

562  
563 Considering the lack of evidence for interference with regulatory networks and the stereoisometry  
564 independent activity of HBD2, we conceived that the observed HBD2 mediated inhibition of biofilm  
565 production is most likely due to embedding in the bacterial membrane and disruption of transport of  
566 biofilm precursor molecules across the membrane. An increasing amount of research suggests that

567 antimicrobial peptides can target discrete loci in bacterial membranes and thereby disrupt biological  
568 processes [109]. For example, antimicrobial peptides are known to impair the assembly of  
569 multicomponent enzyme complexes in the bacterial cell membrane [110] or disrupt periplasmic  
570 protein-protein interaction interfering with molecular transport [111]. In 2013, Kandaswamy and  
571 colleagues showed that HBD2 localizes to the mid-cell region of the Gram-positive bacterium *E.*  
572 *faecalis* [112]. The authors determined that this mid-cell region is rich in anionic phospholipids and  
573 that HBD2 delocalized the spatial organization of protein translocase SecA and sortases, both of  
574 which are important for pilus biogenesis [112; 113]. It is possible that HBD2 targets similar  
575 machinery in *P. aeruginosa* to impair biofilm formation. SecA also plays a role in the transport of  
576 outer membrane proteins in Gram-negative bacteria [114] and outer membrane proteins have been  
577 shown to participate in biofilm formation, including the 11 kDa LecB protein and the 38 kDa OprF  
578 [115; 116]. Consistent with this we found an altered outer membrane protein profile in HBD2 treated  
579 bacteria with a paucity of proteins around 10kDa and proteins around the molecular weights of  
580 previously reported outer membrane proteins. This may indicate structural changes of the outer  
581 membrane, which was further supported by our atomic force microscopy data demonstrating an  
582 increased roughness of the bacterial surface after HBD2 treatment. It is important to note, however,  
583 that increased roughness could also represent changes in the LPS profile. Atomic force microscopy  
584 has been previously employed elsewhere to demonstrate outer membrane damages in *P. aeruginosa*  
585 [117]. Resolving the outer membrane proteins by 2D gel electrophoresis could further delineate the  
586 observed changes in future experiments, which should also revisit the action of the D form of HBD2  
587 and effects on the outer membrane of *A. baumannii*. Finally, outer membrane vesicles have been  
588 recognized to take part in the formation of biofilm by interacting with extracellular DNA and HBD2  
589 interference with proper outer membrane formation may disrupt this process [118].

590  
591 In conclusion, this study reveals distinct activity of two epithelial beta-defensins, HBD2 and HBD3,  
592 and provides evidence for a novel antibacterial action of HBD2. At low concentrations in the  
593 nanomolar range, HBD2 reduced biofilm formation without reducing the metabolic activity of *P.*  
594 *aeruginosa*. Biofilm production of *A. baumannii* was similarly affected, indicating that the observed  
595 HBD2 activity is not strain specific. This activity is unlikely mediated through a receptor-dependent  
596 interference with regulatory networks but contingent on preservation of HBD2 structure. Our  
597 findings are consistent with a membrane-targeted action of HBD2 that affects proper function of  
598 membrane-associated proteins involved in biofilm precursor transport into the extracellular  
599 environment. Future studies dissecting the molecular basis for the described HBD2 activity may  
600 inform the development of new methods for the manipulation of biofilms in aquaculture, in the food  
601 industry, and in the healthcare setting, which is in particular of interest for the latter considering the  
602 rise of multidrug resistance.

#### 603 604 **Conflict of Interest**

605 The authors declare that the research was conducted in the absence of any commercial or financial  
606 relationships that could be construed as a potential conflict of interest.

#### 607 608 **Author Contributions**

609 KRP, BB, TY, MB, EE, ATT, AC, and YW: acquisition of data. KRP, BB, TY, MB, EE, ATT, AC,  
610 HP, YW, WL, and EP: analysis and interpretation of data. KRP, MM, and CA: method development.  
611 KRP and EP: statistical analysis. KRP: molecular docking. KRP, HP, YW, WL, and EP: conceptual  
612 and experimental design. KRP, HP, and EP: drafted manuscript. KRP, BB, TY, MB, EE, ATT, AC,  
613 MM, CA, HP, YW, WL, and EP: critical revision of the manuscript for important intellectual  
614 content. All authors approved the final manuscript submission.

615

**616 Funding**

617 The authors disclosed receipt of the following financial support for the research, authorship, and/or  
618 publication of this article: This work was supported by the National Institutes of Health [grants NIH  
619 SC1 GM096916, NIH RISE GM061331 and NIH LA Basin Bridges to PhD GM054939], the  
620 National Science Foundation [grant NSF-MRI 1828334], the California State University Library  
621 Open Access Author Fund, and the College of Natural and Social Sciences at California State  
622 University Los Angeles [NSS Research and Scholarship Award 2018]. The funders provided no input  
623 to the study design nor in the collection, analyses and interpretation of data.

**625 Acknowledgments**

626 We thank Susan Cohen for helpful discussions. Parts of the result presented here have been included  
627 in the Master's Thesis of KRP [119] and presented at the Microbe 2019 General Meeting of the  
628 American Society for Microbiology in San Francisco, CA, June 20 – 24, 2019.

**631 Contribution to the Field**

632 Biofilms are microbial communities enwrapped in a sticky substance made out of carbohydrates,  
633 proteins, and extracellular DNA. They are formed in water environments but also on body surfaces  
634 where they often precede the development of infectious disease and protect the microbes against host  
635 immune factors and antibiotics. The bacterium *P. aeruginosa* is known to produce biofilms in  
636 patients with a compromised immune system contributing to significant health care burden that is  
637 aggravated by the increasing resistance to antibiotics. Novel approaches to prevent and treat biofilm-  
638 associated infections are needed and innate immune factors that normally prevent infections with *P.*  
639 *aeruginosa* may inform new drug design. Antimicrobial peptides are ancient natural antimicrobial  
640 substances that are widely conserved in nature, underlining their importance for homeostasis. Yet,  
641 different organisms express their own repertoires and antimicrobial peptide expression varies within  
642 an organism pointing to unique localized functions. In this study, we unveil a novel, distinct action of  
643 the epithelial antimicrobial peptide human beta-defensin 2 adding to its known mechanisms of action  
644 and providing a better understanding why immunocompetent individuals are protected against *P.*  
645 *aeruginosa* colonization and infections. This research may lead to the identification of novel targets  
646 for the engineering of antimicrobials.

**648 Data Availability Statement**

649 Datasets are available on request. The raw data supporting the conclusions of this manuscript will be  
650 made available by the authors, without undue reservation, to any qualified researcher.

**653 References**

- 654 [1] P.Y. Qian, S.C. Lau, H.U. Dahms, S. Dobretsov, and T. Harder, Marine biofilms as mediators of  
655 colonization by marine macroorganisms: implications for antifouling and aquaculture. *Marine*  
656 *biotechnology* (New York, N.Y.) 9 (2007) 399-410.
- 657 [2] P.K. Taylor, A.T. Yeung, and R.E. Hancock, Antibiotic resistance in *Pseudomonas aeruginosa*  
658 biofilms: towards the development of novel anti-biofilm therapies. *Journal of biotechnology*  
659 191 (2014) 121-30.
- 660 [3] M. Wilton, L. Charron-Mazenod, R. Moore, and S. Lewenza, Extracellular DNA Acidifies  
661 Biofilms and Induces Aminoglycoside Resistance in *Pseudomonas aeruginosa*. *Antimicrobial*  
662 *agents and chemotherapy* 60 (2016) 544-53.

- 663 [4] R.M. Donlan, and J.W. Costerton, Biofilms: survival mechanisms of clinically relevant  
664 microorganisms. *Clin Microbiol Rev* 15 (2002) 167-93.
- 665 [5] N. Hoiby, T. Bjarnsholt, M. Givskov, S. Molin, and O. Ciofu, Antibiotic resistance of bacterial  
666 biofilms. *International journal of antimicrobial agents* 35 (2010) 322-32.
- 667 [6] L.K. Jennings, K.M. Storek, H.E. Ledvina, C. Coulon, L.S. Marmont, I. Sadovskaya, P.R. Secor,  
668 B.S. Tseng, M. Scian, A. Filloux, D.J. Wozniak, P.L. Howell, and M.R. Parsek, Pel is a  
669 cationic exopolysaccharide that cross-links extracellular DNA in the *Pseudomonas aeruginosa*  
670 biofilm matrix. *Proceedings of the National Academy of Sciences of the United States of*  
671 *America* 112 (2015) 11353-8.
- 672 [7] K.M. Colvin, Y. Irie, C.S. Tart, R. Urbano, J.C. Whitney, C. Ryder, P.L. Howell, D.J. Wozniak,  
673 and M.R. Parsek, The Pel and Psl polysaccharides provide *Pseudomonas aeruginosa* structural  
674 redundancy within the biofilm matrix. *Environmental microbiology* 14 (2012) 1913-28.
- 675 [8] T.B. May, D. Shinabarger, R. Maharaj, J. Kato, L. Chu, J.D. DeVault, S. Roychoudhury, N.A.  
676 Zielinski, A. Berry, R.K. Rothmel, and et al., Alginate synthesis by *Pseudomonas aeruginosa*:  
677 a key pathogenic factor in chronic pulmonary infections of cystic fibrosis patients. *Clin*  
678 *Microbiol Rev* 4 (1991) 191-206.
- 679 [9] J.N.C. Fong, and F.H. Yildiz, Biofilm Matrix Proteins. *Microbiology spectrum* 3 (2015).
- 680 [10] L. Turnbull, M. Toyofuku, A.L. Hynen, M. Kurosawa, G. Pessi, N.K. Petty, S.R. Osvath, G.  
681 Carcamo-Oyarce, E.S. Gloag, R. Shimoni, U. Omasits, S. Ito, X. Yap, L.G. Monahan, R.  
682 Cavaliere, C.H. Ahrens, I.G. Charles, N. Nomura, L. Eberl, and C.B. Whitchurch, Explosive  
683 cell lysis as a mechanism for the biogenesis of bacterial membrane vesicles and biofilms.  
684 *Nature communications* 7 (2016) 11220.
- 685 [11] C.B. Whitchurch, T. Tolker-Nielsen, P.C. Ragas, and J.S. Mattick, Extracellular DNA required  
686 for bacterial biofilm formation. *Science (New York, N.Y.)* 295 (2002) 1487.
- 687 [12] T. Das, S. Sehar, and M. Manefield, The roles of extracellular DNA in the structural integrity of  
688 extracellular polymeric substance and bacterial biofilm development. *Environmental*  
689 *microbiology reports* 5 (2013) 778-86.
- 690 [13] O.E. Petrova, and K. Sauer, Sticky situations: key components that control bacterial surface  
691 attachment. *Journal of bacteriology* 194 (2012) 2413-25.
- 692 [14] B. Stojkovic, S. Sretenovic, I. Dogsa, I. Poberaj, and D. Stopar, Viscoelastic properties of levan-  
693 DNA mixtures important in microbial biofilm formation as determined by micro- and  
694 macrorheology. *Biophysical journal* 108 (2015) 758-65.
- 695 [15] K.N. Cowles, and Z. Gitai, Surface association and the MreB cytoskeleton regulate pilus  
696 production, localization and function in *Pseudomonas aeruginosa*. *Molecular microbiology* 76  
697 (2010) 1411-26.
- 698 [16] J.P. Pearson, L. Passador, B.H. Iglewski, and E.P. Greenberg, A second N-acylhomoserine  
699 lactone signal produced by *Pseudomonas aeruginosa*. *Proceedings of the National Academy*  
700 *of Sciences of the United States of America* 92 (1995) 1490-4.
- 701 [17] G. Laverty, S.P. Gorman, and B.F. Gilmore, Biomolecular Mechanisms of *Pseudomonas*  
702 *aeruginosa* and *Escherichia coli* Biofilm Formation. *Pathogens* 3 (2014) 596-632.
- 703 [18] S.T. Rutherford, and B.L. Bassler, Bacterial quorum sensing: its role in virulence and  
704 possibilities for its control. *Cold Spring Harbor perspectives in medicine* 2 (2012).

- 705 [19] J. Overhage, M. Schemionek, J.S. Webb, and B.H. Rehm, Expression of the *psl* operon in  
706 *Pseudomonas aeruginosa* PAO1 biofilms: PslA performs an essential function in biofilm  
707 formation. *Applied and environmental microbiology* 71 (2005) 4407-13.
- 708 [20] Y. Irie, M. Starkey, A.N. Edwards, D.J. Wozniak, T. Romeo, and M.R. Parsek, *Pseudomonas*  
709 *aeruginosa* biofilm matrix polysaccharide Psl is regulated transcriptionally by RpoS and post-  
710 transcriptionally by RsmA. *Molecular microbiology* 78 (2010) 158-72.
- 711 [21] A.R. Hauser, The type III secretion system of *Pseudomonas aeruginosa*: infection by injection.  
712 *Nature reviews. Microbiology* 7 (2009) 654-65.
- 713 [22] L. Zulianello, C. Canard, T. Kohler, D. Caille, J.S. Lacroix, and P. Meda, Rhamnolipids are  
714 virulence factors that promote early infiltration of primary human airway epithelia by  
715 *Pseudomonas aeruginosa*. *Infection and immunity* 74 (2006) 3134-47.
- 716 [23] Z. Hosseinidou, N. Tufenkji, and T.G. van de Ven, Predation in homogeneous and  
717 heterogeneous phage environments affects virulence determinants of *Pseudomonas*  
718 *aeruginosa*. *Applied and environmental microbiology* 79 (2013) 2862-71.
- 719 [24] V. Naik, and G. Mahajan, Quorum sensing: a non-conventional target for antibiotic discovery.  
720 *Natural product communications* 8 (2013) 1455-8.
- 721 [25] V.T. Orlandi, F. Bolognese, L. Chiodaroli, T. Tolker-Nielsen, and P. Barbieri, Pigments  
722 influence the tolerance of *Pseudomonas aeruginosa* PAO1 to photodynamically induced  
723 oxidative stress. *Microbiology* 161 (2015) 2298-309.
- 724 [26] J.A. Driscoll, S.L. Brody, and M.H. Kollef, The epidemiology, pathogenesis and treatment of  
725 *Pseudomonas aeruginosa* infections. *Drugs* 67 (2007) 351-68.
- 726 [27] M. Zasloff, Antibiotic peptides as mediators of innate immunity. *Current opinion in*  
727 *immunology* 4 (1992) 3-7.
- 728 [28] C.L. Bevins, Antimicrobial peptides as effector molecules of mammalian host defense.  
729 *Contributions to microbiology* 10 (2003) 106-48.
- 730 [29] E. Martin, T. Ganz, and R.I. Lehrer, Defensins and other endogenous peptide antibiotics of  
731 vertebrates. *Journal of leukocyte biology* 58 (1995) 128-36.
- 732 [30] A. Oren, T. Ganz, L. Liu, and T. Meerloo, In human epidermis, beta-defensin 2 is packaged in  
733 lamellar bodies. *Experimental and molecular pathology* 74 (2003) 180-2.
- 734 [31] L. Liu, L. Wang, H.P. Jia, C. Zhao, H.H. Heng, B.C. Schutte, P.B. McCray, Jr., and T. Ganz,  
735 Structure and mapping of the human beta-defensin HBD-2 gene and its expression at sites of  
736 inflammation. *Gene* 222 (1998) 237-44.
- 737 [32] C.J. Hertz, Q. Wu, E.M. Porter, Y.J. Zhang, K.H. Weismuller, P.J. Godowski, T. Ganz, S.H.  
738 Randell, and R.L. Modlin, Activation of Toll-like receptor 2 on human tracheobronchial  
739 epithelial cells induces the antimicrobial peptide human beta defensin-2. *Journal of*  
740 *immunology* (Baltimore, Md. : 1950) 171 (2003) 6820-6.
- 741 [33] G. Wang, Human antimicrobial peptides and proteins. *Pharmaceuticals* (Basel, Switzerland) 7  
742 (2014) 545-94.
- 743 [34] K. Matsuzaki, Membrane Permeabilization Mechanisms. *Advances in experimental medicine*  
744 *and biology* 1117 (2019) 9-16.



- 745 [35] J.C. Bozelli, Jr., E.T. Sasahara, M.R. Pinto, C.R. Nakaie, and S. Schreier, Effect of head group  
746 and curvature on binding of the antimicrobial peptide tritrpticin to lipid membranes.  
747 *Chemistry and physics of lipids* 165 (2012) 365-73.
- 748 [36] E. Strandberg, D. Tiltak, S. Ehni, P. Wadhvani, and A.S. Ulrich, Lipid shape is a key factor for  
749 membrane interactions of amphipathic helical peptides. *Biochimica et biophysica acta* 1818  
750 (2012) 1764-76.
- 751 [37] E. Strandberg, J. Zerweck, P. Wadhvani, and A.S. Ulrich, Synergistic insertion of antimicrobial  
752 magainin-family peptides in membranes depends on the lipid spontaneous curvature.  
753 *Biophysical journal* 104 (2013) L9-11.
- 754 [38] S. Afonin, R.W. Glaser, C. Sachse, J. Salgado, P. Wadhvani, and A.S. Ulrich, (19)F NMR  
755 screening of unrelated antimicrobial peptides shows that membrane interactions are largely  
756 governed by lipids. *Biochimica et biophysica acta* 1838 (2014) 2260-8.
- 757 [39] B.S. Perrin, Jr., A.J. Sodt, M.L. Cotten, and R.W. Pastor, The Curvature Induction of Surface-  
758 Bound Antimicrobial Peptides Piscidin 1 and Piscidin 3 Varies with Lipid Chain Length. *The*  
759 *Journal of membrane biology* 248 (2015) 455-67.
- 760 [40] D.J. Paterson, M. Tassieri, J. Reboud, R. Wilson, and J.M. Cooper, Lipid topology and  
761 electrostatic interactions underpin lytic activity of linear cationic antimicrobial peptides in  
762 membranes. *Proceedings of the National Academy of Sciences of the United States of*  
763 *America* 114 (2017) E8324-e8332.
- 764 [41] K.A. Brogden, Antimicrobial peptides: pore formers or metabolic inhibitors in bacteria? *Nature*  
765 *reviews. Microbiology* 3 (2005) 238-50.
- 766 [42] A. Fabisiak, N. Murawska, and J. Fichna, LL-37: Cathelicidin-related antimicrobial peptide with  
767 pleiotropic activity. *Pharmacological reports : PR* 68 (2016) 802-8.
- 768 [43] J. Overhage, A. Campisano, M. Bains, E.C. Torfs, B.H. Rehm, and R.E. Hancock, Human host  
769 defense peptide LL-37 prevents bacterial biofilm formation. *Infection and immunity* 76  
770 (2008) 4176-82.
- 771 [44] C. Nagant, B. Pitts, K. Nazmi, M. Vandenbranden, J.G. Bolscher, P.S. Stewart, and J.P. Dehaye,  
772 Identification of peptides derived from the human antimicrobial peptide LL-37 active against  
773 biofilms formed by *Pseudomonas aeruginosa* using a library of truncated fragments.  
774 *Antimicrobial agents and chemotherapy* 56 (2012) 5698-708.
- 775 [45] C. Koro, A. Hellvard, N. Delaleu, V. Binder, C. Scavenius, B. Bergum, I. Glowczyk, H.M.  
776 Roberts, I.L. Chapple, M.M. Grant, M. Rapala-Kozik, K. Kлага, J.J. Enghild, J. Potempa, and  
777 P. Mydel, Carbamylated LL-37 as a modulator of the immune response. *Innate immunity* 22  
778 (2016) 218-29.
- 779 [46] Y. Kai-Larsen, and B. Agerberth, The role of the multifunctional peptide LL-37 in host defense.  
780 *Frontiers in bioscience : a journal and virtual library* 13 (2008) 3760-7.
- 781 [47] V. Sass, T. Schneider, M. Wilmes, C. Korner, A. Tossi, N. Novikova, O. Shamova, and H.G.  
782 Sahl, Human beta-defensin 3 inhibits cell wall biosynthesis in *Staphylococci*. *Infection and*  
783 *immunity* 78 (2010) 2793-800.
- 784 [48] N. Kanda, M. Kamata, Y. Tada, T. Ishikawa, S. Sato, and S. Watanabe, Human beta-defensin-2  
785 enhances IFN-gamma and IL-10 production and suppresses IL-17 production in T cells.  
786 *Journal of leukocyte biology* 89 (2011) 935-44.

- 787 [49] A.B. Estrela, M. Rohde, M.G. Gutierrez, G. Molinari, and W.R. Abraham, Human beta-defensin  
788 2 induces extracellular accumulation of adenosine in Escherichia coli. *Antimicrobial agents*  
789 *and chemotherapy* 57 (2013) 4387-93.
- 790 [50] D. Yang, O. Chertov, S.N. Bykovskaia, Q. Chen, M.J. Buffo, J. Shogan, M. Anderson, J.M.  
791 Schroder, J.M. Wang, O.M. Howard, and J.J. Oppenheim, Beta-defensins: linking innate and  
792 adaptive immunity through dendritic and T cell CCR6. *Science (New York, N.Y.)* 286 (1999)  
793 525-8.
- 794 [51] B. Spudy, F.D. Sonnichsen, G.H. Waetzig, J. Grotzinger, and S. Jung, Identification of structural  
795 traits that increase the antimicrobial activity of a chimeric peptide of human beta-defensins 2  
796 and 3. *Biochemical and biophysical research communications* 427 (2012) 207-11.
- 797 [52] D.M. Hoover, Z. Wu, K. Tucker, W. Lu, and J. Lubkowski, Antimicrobial characterization of  
798 human beta-defensin 3 derivatives. *Antimicrobial agents and chemotherapy* 47 (2003) 2804-  
799 9.
- 800 [53] V. Dhople, A. Krukemeyer, and A. Ramamoorthy, The human beta-defensin-3, an antibacterial  
801 peptide with multiple biological functions. *Biochimica et biophysica acta* 1758 (2006) 1499-  
802 512.
- 803 [54] O.N. Silva, W.F. Porto, S.M. Ribeiro, I. Batista, and O.L. Franco, Host-defense peptides and  
804 their potential use as biomarkers in human diseases. *Drug discovery today* 23 (2018) 1666-  
805 1671.
- 806 [55] E. Galdiero, L. Lombardi, A. Falanga, G. Libralato, M. Guida, and R. Carotenuto, Biofilms:  
807 Novel Strategies Based on Antimicrobial Peptides. *Pharmaceutics* 11 (2019).
- 808 [56] Z. Wu, D.M. Hoover, D. Yang, C. Boulegue, F. Santamaria, J.J. Oppenheim, J. Lubkowski, and  
809 W. Lu, Engineering disulfide bridges to dissect antimicrobial and chemotactic activities of  
810 human beta-defensin 3. *Proceedings of the National Academy of Sciences of the United*  
811 *States of America* 100 (2003) 8880-5.
- 812 [57] G. Wei, E. de Leeuw, M. Pazgier, W. Yuan, G. Zou, J. Wang, B. Ericksen, W.Y. Lu, R.I.  
813 Lehrer, and W. Lu, Through the looking glass, mechanistic insights from enantiomeric human  
814 defensins. *The Journal of biological chemistry* 284 (2009) 29180-92.
- 815 [58] J.H. Merritt, D.E. Kadouri, and G.A. O'Toole, Growing and analyzing static biofilms. *Current*  
816 *protocols in microbiology* Chapter 1 (2005) Unit 1B.1.
- 817 [59] M.U. Shiloh, J. Ruan, and C. Nathan, Evaluation of bacterial survival and phagocyte function  
818 with a fluorescence-based microplate assay. *Infection and immunity* 65 (1997) 3193-8.
- 819 [60] J.G. Martinez, M. Waldon, Q. Huang, S. Alvarez, A. Oren, N. Sandoval, M. Du, F. Zhou, A.  
820 Zenz, K. Lohner, R. Desharnais, and E. Porter, Membrane-targeted synergistic activity of  
821 docosahexaenoic acid and lysozyme against *Pseudomonas aeruginosa*. *The Biochemical*  
822 *journal* 419 (2009) 193-200.
- 823 [61] E.A. Abu, S. Su, L. Sallans, R.E. Boissy, A. Greatens, W.R. Heineman, and D.J. Hassett, Cyclic  
824 voltammetric, fluorescence and biological analysis of purified aeruginosin A, a secreted red  
825 pigment of *Pseudomonas aeruginosa* PAO1. *Microbiology* 159 (2013) 1736-47.
- 826 [62] S. Shityakov, and C. Forster, In silico predictive model to determine vector-mediated transport  
827 properties for the blood-brain barrier choline transporter. *Advances and applications in*  
828 *bioinformatics and chemistry : AABC* 7 (2014) 23-36.

- 829 [63] M. Park, G. Yoo, J.H. Bong, J. Jose, M.J. Kang, and J.C. Pyun, Isolation and characterization of  
830 the outer membrane of *Escherichia coli* with autodeployed Z-domains. *Biochimica et*  
831 *biophysica acta* 1848 (2015) 842-7.
- 832 [64] Y. Chao, and T. Zhang, Optimization of fixation methods for observation of bacterial cell  
833 morphology and surface ultrastructures by atomic force microscopy. *Appl Microbiol*  
834 *Biotechnol* 92 (2011) 381-92.
- 835 [65] Y.F. Dufrene, T. Ando, R. Garcia, D. Alsteens, D. Martinez-Martin, A. Engel, C. Gerber, and  
836 D.J. Muller, Imaging modes of atomic force microscopy for application in molecular and cell  
837 biology. *Nature nanotechnology* 12 (2017) 295-307.
- 838 [66] J. Rohrl, D. Yang, J.J. Oppenheim, and T. Hehlhans, Human beta-defensin 2 and 3 and their  
839 mouse orthologs induce chemotaxis through interaction with CCR2. *Journal of immunology*  
840 (Baltimore, Md. : 1950) 184 (2010) 6688-94.
- 841 [67] J. Rohrl, D. Yang, J.J. Oppenheim, and T. Hehlhans, Specific binding and chemotactic activity  
842 of mBD4 and its functional orthologue hBD2 to CCR6-expressing cells. *The Journal of*  
843 *biological chemistry* 285 (2010) 7028-34.
- 844 [68] D.M. Hoover, K.R. Rajashankar, R. Blumenthal, A. Puri, J.J. Oppenheim, O. Chertov, and J.  
845 Lubkowski, The structure of human beta-defensin-2 shows evidence of higher order  
846 oligomerization. *The Journal of biological chemistry* 275 (2000) 32911-8.
- 847 [69] M.V. Trivedi, J.S. Laurence, and T.J. Siahaan, The role of thiols and disulfides on protein  
848 stability. *Current protein & peptide science* 10 (2009) 614-25.
- 849 [70] J.N. Onuchic, Z. Luthey-Schulten, and P.G. Wolynes, Theory of protein folding: the energy  
850 landscape perspective. *Annual review of physical chemistry* 48 (1997) 545-600.
- 851 [71] P.N. Jimenez, G. Koch, J.A. Thompson, K.B. Xavier, R.H. Cool, and W.J. Quax, The multiple  
852 signaling systems regulating virulence in *Pseudomonas aeruginosa*. *Microbiology and*  
853 *molecular biology reviews* : MMBR 76 (2012) 46-65.
- 854 [72] Y. Zou, and S.K. Nair, Molecular basis for the recognition of structurally distinct autoinducer  
855 mimics by the *Pseudomonas aeruginosa* LasR quorum-sensing signaling receptor. *Chemistry*  
856 *& biology* 16 (2009) 961-70.
- 857 [73] C.F. Le, M.Y. Yusof, M.A. Hassan, V.S. Lee, D.M. Isa, and S.D. Sekaran, In vivo efficacy and  
858 molecular docking of designed peptide that exhibits potent antipneumococcal activity and  
859 synergises in combination with penicillin. *Scientific reports* 5 (2015) 11886.
- 860 [74] J.D. Moore, F.M. Rossi, M.A. Welsh, K.E. Nyffeler, and H.E. Blackwell, A Comparative  
861 Analysis of Synthetic Quorum Sensing Modulators in *Pseudomonas aeruginosa*: New Insights  
862 into Mechanism, Active Efflux Susceptibility, Phenotypic Response, and Next-Generation  
863 Ligand Design. *Journal of the American Chemical Society* 137 (2015) 14626-39.
- 864 [75] I.J. Choi, C.S. Rhee, C.H. Lee, and D.Y. Kim, Effect of allergic rhinitis on the expression of  
865 human beta-defensin 2 in tonsils. *Annals of allergy, asthma & immunology* : official  
866 publication of the American College of Allergy, Asthma, & Immunology 110 (2013) 178-83.
- 867 [76] T. Hiratsuka, M. Nakazato, Y. Date, J. Ashitani, T. Minematsu, N. Chino, and S. Matsukura,  
868 Identification of human beta-defensin-2 in respiratory tract and plasma and its increase in  
869 bacterial pneumonia. *Biochemical and biophysical research communications* 249 (1998) 943-  
870 7.

- 871 [77] T. Hiratsuka, H. Mukae, H. Iiboshi, J. Ashitani, K. Nabeshima, T. Minematsu, N. Chino, T. Ihi,  
872 S. Kohno, and M. Nakazato, Increased concentrations of human beta-defensins in plasma and  
873 bronchoalveolar lavage fluid of patients with diffuse panbronchiolitis. *Thorax* 58 (2003) 425-  
874 30.
- 875 [78] S. Chevalier, E. Bouffartigues, J. Bodilis, O. Maillot, O. Lesouhaitier, M.G.J. Feuilloley, N.  
876 Orange, A. Dufour, and P. Cornelis, Structure, function and regulation of *Pseudomonas*  
877 *aeruginosa* porins. *FEMS microbiology reviews* 41 (2017) 698-722.
- 878 [79] R.E. Hancock, R. Siehnel, and N. Martin, Outer membrane proteins of *Pseudomonas*. *Molecular*  
879 *microbiology* 4 (1990) 1069-75.
- 880 [80] J.E. Goeke, S. Kist, S. Schubert, R. Hickel, K.C. Huth, and M. Kollmuss, Sensitivity of caries  
881 pathogens to antimicrobial peptides related to caries risk. *Clinical oral investigations* 22  
882 (2018) 2519-2525.
- 883 [81] D.A. O'Neil, S.P. Cole, E. Martin-Porter, M.P. Housley, L. Liu, T. Ganz, and M.F. Kagnoff,  
884 Regulation of human beta-defensins by gastric epithelial cells in response to infection with  
885 *Helicobacter pylori* or stimulation with interleukin-1. *Infection and immunity* 68 (2000) 5412-  
886 5.
- 887 [82] A. Crabbe, L. Ostyn, S. Staelens, C. Rigauts, M. Risseuw, M. Dhaenens, S. Daled, H. Van  
888 Acker, D. Deforce, S. Van Calenbergh, and T. Coenye, Host metabolites stimulate the  
889 bacterial proton motive force to enhance the activity of aminoglycoside antibiotics. *PLoS*  
890 *pathogens* 15 (2019) e1007697.
- 891 [83] K.M. Scherer, J.H. Spille, H.G. Sahl, F. Grein, and U. Kubitscheck, The lantibiotic nisin induces  
892 lipid II aggregation, causing membrane instability and vesicle budding. *Biophysical journal*  
893 108 (2015) 1114-24.
- 894 [84] C. van Kraaij, E. Breukink, M.A. Noordermeer, R.A. Demel, R.J. Siezen, O.P. Kuipers, and B.  
895 de Kruijff, Pore formation by nisin involves translocation of its C-terminal part across the  
896 membrane. *Biochemistry* 37 (1998) 16033-40.
- 897 [85] K. Winkowski, R.D. Ludescher, and T.J. Montville, Physicochemical characterization of the  
898 nisin-membrane interaction with liposomes derived from *Listeria monocytogenes*. *Applied*  
899 *and environmental microbiology* 62 (1996) 323-7.
- 900 [86] M.J. Garcera, M.G. Elferink, A.J. Driessen, and W.N. Konings, In vitro pore-forming activity of  
901 the lantibiotic nisin. Role of protonmotive force and lipid composition. *European journal of*  
902 *biochemistry / FEBS* 212 (1993) 417-22.
- 903 [87] G. Bierbaum, and H.G. Sahl, Lantibiotics: mode of action, biosynthesis and bioengineering.  
904 *Current pharmaceutical biotechnology* 10 (2009) 2-18.
- 905 [88] E. de Leeuw, C. Li, P. Zeng, C. Li, M. Diepeveen-de Buin, W.Y. Lu, E. Breukink, and W. Lu,  
906 Functional interaction of human neutrophil peptide-1 with the cell wall precursor lipid II.  
907 *FEBS letters* 584 (2010) 1543-8.
- 908 [89] D.J. Schibli, H.N. Hunter, V. Aseyev, T.D. Starner, J.M. Wiencek, P.B. McCray, Jr., B.F. Tack,  
909 and H.J. Vogel, The solution structures of the human beta-defensins lead to a better  
910 understanding of the potent bactericidal activity of HBD3 against *Staphylococcus aureus*. *The*  
911 *Journal of biological chemistry* 277 (2002) 8279-89.
- 912 [90] C. Chan, L.L. Burrows, and C.M. Deber, Helix induction in antimicrobial peptides by alginate in  
913 biofilms. *The Journal of biological chemistry* 279 (2004) 38749-54.

- 914 [91] C. Perez-Cruz, L. Delgado, C. Lopez-Iglesias, and E. Mercade, Outer-inner membrane vesicles  
915 naturally secreted by gram-negative pathogenic bacteria. *PloS one* 10 (2015) e0116896.
- 916 [92] B. Mathew, and R. Nagaraj, Antimicrobial activity of human alpha-defensin 6 analogs: insights  
917 into the physico-chemical reasons behind weak bactericidal activity of HD6 in vitro. *J Pept*  
918 *Sci* 21 (2015) 811-8.
- 919 [93] K.B. Chandrababu, B. Ho, and D. Yang, Structure, dynamics, and activity of an all-cysteine  
920 mutated human beta defensin-3 peptide analogue. *Biochemistry* 48 (2009) 6052-61.
- 921 [94] V. Krishnakumari, and R. Nagaraj, Interaction of antibacterial peptides spanning the carboxy-  
922 terminal region of human beta-defensins 1-3 with phospholipids at the air-water interface and  
923 inner membrane of *E. coli*. *Peptides* 29 (2008) 7-14.
- 924 [95] L. Mashburn-Warren, J. Howe, P. Garidel, W. Richter, F. Steiniger, M. Roessle, K.  
925 Brandenburg, and M. Whiteley, Interaction of quorum signals with outer membrane lipids:  
926 insights into prokaryotic membrane vesicle formation. *Molecular microbiology* 69 (2008)  
927 491-502.
- 928 [96] A.R. McCready, J.E. Paczkowski, B.R. Henke, and B.L. Bassler, Structural determinants driving  
929 homoserine lactone ligand selection in the *Pseudomonas aeruginosa* LasR quorum-sensing  
930 receptor. *Proceedings of the National Academy of Sciences of the United States of America*  
931 116 (2019) 245-254.
- 932 [97] T.J. Tavender, N.M. Halliday, K.R. Hardie, and K. Winzer, LuxS-independent formation of AI-  
933 2 from ribulose-5-phosphate. *BMC microbiology* 8 (2008) 98.
- 934 [98] H. Li, X. Li, Z. Wang, Y. Fu, Q. Ai, Y. Dong, and J. Yu, Autoinducer-2 regulates *Pseudomonas*  
935 *aeruginosa* PAO1 biofilm formation and virulence production in a dose-dependent manner.  
936 *BMC microbiology* 15 (2015) 192.
- 937 [99] M.B. Miller, and B.L. Bassler, Quorum sensing in bacteria. *Annual review of microbiology* 55  
938 (2001) 165-99.
- 939 [100] K. Duan, C. Dammel, J. Stein, H. Rabin, and M.G. Surette, Modulation of *Pseudomonas*  
940 *aeruginosa* gene expression by host microflora through interspecies communication.  
941 *Molecular microbiology* 50 (2003) 1477-91.
- 942 [101] Q. Wei, and L.Z. Ma, Biofilm matrix and its regulation in *Pseudomonas aeruginosa*.  
943 *International journal of molecular sciences* 14 (2013) 20983-1005.
- 944 [102] H. Mikkelsen, M. Sivaneson, and A. Filloux, Key two-component regulatory systems that  
945 control biofilm formation in *Pseudomonas aeruginosa*. *Environmental microbiology* 13  
946 (2011) 1666-81.
- 947 [103] D.G. Ha, and G.A. O'Toole, c-di-GMP and its Effects on Biofilm Formation and Dispersion: a  
948 *Pseudomonas Aeruginosa* Review. *Microbiology spectrum* 3 (2015) Mb-0003-2014.
- 949 [104] C. de la Fuente-Nunez, F. Reffuveille, E.F. Haney, S.K. Straus, and R.E. Hancock, Broad-  
950 spectrum anti-biofilm peptide that targets a cellular stress response. *PLoS pathogens* 10  
951 (2014) e1004152.
- 952 [105] L. Steinstraesser, T. Hirsch, M. Schulte, M. Kueckelhaus, F. Jacobsen, E.A. Mersch, I.  
953 Stricker, N. Afacan, H. Jenssen, R.E. Hancock, and J. Kindrachuk, Innate defense regulator  
954 peptide 1018 in wound healing and wound infection. *PloS one* 7 (2012) e39373.

- 955 [106] G.S. Byng, D.C. Eustice, and R.A. Jensen, Biosynthesis of phenazine pigments in mutant and  
956 wild-type cultures of *Pseudomonas aeruginosa*. *Journal of bacteriology* 138 (1979) 846-52.
- 957 [107] A. Bala, L. Kumar, S. Chhibber, and K. Harjai, Augmentation of virulence related traits of pqs  
958 mutants by *Pseudomonas* quinolone signal through membrane vesicles. *Journal of basic*  
959 *microbiology* 55 (2015) 566-78.
- 960 [108] Y.L. Lo, L. Shen, C.H. Chang, M. Bhuwan, C.H. Chiu, and H.Y. Chang, Regulation of  
961 Motility and Phenazine Pigment Production by FliA Is Cyclic-di-GMP Dependent in  
962 *Pseudomonas aeruginosa* PAO1. *PloS one* 11 (2016) e0155397.
- 963 [109] R. Rashid, M. Veleba, and K.A. Kline, Focal Targeting of the Bacterial Envelope by  
964 Antimicrobial Peptides. *Frontiers in cell and developmental biology* 4 (2016) 55.
- 965 [110] M. Wenzel, A.I. Chiriac, A. Otto, D. Zweytick, C. May, C. Schumacher, R. Gust, H.B. Albada,  
966 M. Penkova, U. Kramer, R. Erdmann, N. Metzler-Nolte, S.K. Straus, E. Bremer, D. Becher,  
967 H. Brotz-Oesterhelt, H.G. Sahl, and J.E. Bandow, Small cationic antimicrobial peptides  
968 delocalize peripheral membrane proteins. *Proceedings of the National Academy of Sciences*  
969 *of the United States of America* 111 (2014) E1409-18.
- 970 [111] S.U. Vetterli, K. Zerbe, M. Muller, M. Urfer, M. Mondal, S.Y. Wang, K. Moehle, O. Zerbe, A.  
971 Vitale, G. Pessi, L. Eberl, B. Wollscheid, and J.A. Robinson, Thanatin targets the  
972 intermembrane protein complex required for lipopolysaccharide transport in *Escherichia coli*.  
973 *Science advances* 4 (2018) eaau2634.
- 974 [112] K. Kandaswamy, T.H. Liew, C.Y. Wang, E. Huston-Warren, U. Meyer-Hoffert, K. Hultenby,  
975 J.M. Schroder, M.G. Caparon, S. Normark, B. Henriques-Normark, S.J. Hultgren, and K.A.  
976 Kline, Focal targeting by human beta-defensin 2 disrupts localized virulence factor assembly  
977 sites in *Enterococcus faecalis*. *Proceedings of the National Academy of Sciences of the*  
978 *United States of America* 110 (2013) 20230-5.
- 979 [113] H.V. Nielsen, A.L. Flores-Mireles, A.L. Kau, K.A. Kline, J.S. Pinkner, F. Neiers, S. Normark,  
980 B. Henriques-Normark, M.G. Caparon, and S.J. Hultgren, Pilin and sortase residues critical  
981 for endocarditis- and biofilm-associated pilus biogenesis in *Enterococcus faecalis*. *Journal of*  
982 *bacteriology* 195 (2013) 4484-95.
- 983 [114] Q. Ma, Y. Zhai, J.C. Schneider, T.M. Ramseier, and M.H. Saier, Jr., Protein secretion systems  
984 of *Pseudomonas aeruginosa* and *P fluorescens*. *Biochimica et biophysica acta* 1611 (2003)  
985 223-33.
- 986 [115] D. Tielker, S. Hacker, R. Loris, M. Strathmann, J. Wingender, S. Wilhelm, F. Rosenau, and  
987 K.E. Jaeger, *Pseudomonas aeruginosa* lectin LecB is located in the outer membrane and is  
988 involved in biofilm formation. *Microbiology* 151 (2005) 1313-1323.
- 989 [116] E.K. Cassin, and B.S. Tseng, Pushing beyond the envelope: the potential roles of OprF in  
990 *Pseudomonas aeruginosa* biofilm formation and pathogenicity. *Journal of bacteriology*  
991 (2019).
- 992 [117] A. Li, P.Y. Lee, B. Ho, J.L. Ding, and C.T. Lim, Atomic force microscopy study of the  
993 antimicrobial action of Sushi peptides on Gram negative bacteria. *Biochimica et biophysica*  
994 *acta* 1768 (2007) 411-8.
- 995 [118] S.R. Schooling, A. Hubble, and T.J. Beveridge, Interactions of DNA with biofilm-derived  
996 membrane vesicles. *Journal of bacteriology* 191 (2009) 4097-102.

- 997 [119] K.M.R. Parducho, Airway Peptides and Lipids- Effects on *Pseudomonas aeruginosa*  
998 Morphology, Biofilm Formation, and Quorum Sensing, Chemistry & Biochemistry,  
999 California State University Los Angeles, Los Angeles, 2018.
- 1000 [120] J. Kyte, and R.F. Doolittle, A simple method for displaying the hydrophobic character of a  
1001 protein. *Journal of molecular biology* 157 (1982) 105-32.
- 1002 [121] W.C. Wimley, and S.H. White, Experimentally determined hydrophobicity scale for proteins at  
1003 membrane interfaces. *Nature structural biology* 3 (1996) 842-8.
- 1004

1005 **Tables**1006 **Table 1.** Human Beta Defensins-2 and -3 physicochemical properties.

Peptide	Amino acid sequence <sup>a</sup>	MW (Da)	Net Charge	Hydrophobicity index	
				Kyte-Doolittle <sup>b</sup>	Wimley-White <sup>c</sup>
HBD2	GIGDPVTC <sup>1</sup> LKSGAIC <sup>2</sup> HPVFC <sup>3</sup> PRRY KQIGTC <sup>2</sup> GLPGTKC <sup>1</sup> C <sup>3</sup> KKP	4,328.22	6	-0.1	6.16
Linear HBD2	GIGDPVTALKSGAIAHPVFA <sup>1</sup> PRRYK QIGTAGLPGTKA <sup>1</sup> AKKP	4,141.88	6	-0.21	8.62
HBD3	GIINTLQKYYC <sup>1</sup> RVRGGRC <sup>2</sup> AVLSC <sup>3</sup> LPKEEQIGKC <sup>2</sup> STRGRKC <sup>1</sup> C <sup>3</sup> RRKK	5,155.19	11	-0.7	12.65

1007 <sup>a</sup> Amino acid sequences are given in one-letter code starting from the N and ending with the C terminus. Underlined  
 1008 residues denote mutation sites for the linearized HBD2. Cationic residues are in boldface. Anionic residues are italicized.

1009 <sup>b</sup> Values were calculated based on the Kyte-Doolittle hydrophobicity scale [120] using the grand average of hydropathy  
 1010 (GRAVY) program. Higher values represent an increase in hydrophobicity.

1011 <sup>c</sup> Values were calculated based on the Wimley-White whole residue hydrophobicity interface scale (Wimley & White  
 1012 1996) [121] using the APD3 antimicrobial peptide calculator and predictor. Lower values represent an increase in  
 1013 hydrophobicity.

1014 <sup>1-3</sup> Numbers denote disulfide bond connectivity.

1015

1016

1017 **Table 2.** Primers used in this study.

Gene target		5' - 3' Sequence	T <sub>m</sub> (°C)	Product size (bp)	Product melt peak (°C)
<i>pslA</i>	F	CGTTCTGCCTGCTGTTGTTC	56.9	160	88.5
	R	TACATGCCGCGTTTCATCCA	57.3		
<i>gapA</i>	F	CCATCGGATCGTCTCGAA	61.0	130	88.0
	R	GTTCTGGTCGTTGGTGTAG	60.0		
<i>flgF</i>	F	ACAACCTGGCGAACATCTC	62.0	137	89.0
	R	GCCATGGCTGAAATCGGTA	62.0		

1018



1019 **Table 3.** Dissociation constants for quorum sensing molecules calculated using AutoDock Vina  
1020 measurements. The best binding energies (predicted by AutoDock Vina) for each ligand-receptor pair  
1021 were used to manually calculate dissociation constants ( $K_D$ ) using Equation [1]. NEtP:  
1022 phosphorylcolamine; 3-oxo-C12-HSL: N-(3-oxododecanoyl) homoserine lactone; C4-HSL: N-  
1023 butanoyl homoserine lactone; PQS: 2-heptyl-3-hydroxy-4-quinolone.  
1024

Receptor	NEtP	3-oxo-C12--HSL	C4-HSL	PQS <sub>t</sub>
LasR	558 $\mu$ M	1.15 $\mu$ M	18.3 $\mu$ M	191 nM
HBD2	4.637 mM	3.348 mM	2.417 mM	403 $\mu$ M

1025

1026

1027 **Figure Legends**1028 **Figure 1**1029 **Metabolic activity of *P. aeruginosa* in the presence and absence of HBD2 and HBD3 over 18 h.**

1030 Bacteria were incubated in 10% Mueller-Hinton/140 mM NaCl supplemented with 0.01 % resazurin  
1031 and fluorescence emitted by resorufin reflecting the production of reducing metabolites was  
1032 measured every 3 h (530 nm<sub>ex</sub>, 616 nm<sub>em</sub>). Shown are the means ± SD of three independent  
1033 experiments conducted in duplicates. RFU: relative fluorescence units.  $p < 0.001$  for HBD2 (A) at 1,  
1034 2, and 4 μM and for HBD3 (B) at 0.25, 0.5, and 1 μM compared to the solvent control in univariate  
1035 ANOVA with Bonferroni posthoc analysis. All other concentrations were not significantly different  
1036 from the solvent controls.

1037 **Figure 2**1038 **Comparative effects of HBD2 and HBD3 on *P. aeruginosa* biofilm and metabolic activity.**

1039 Shown are biofilm formation and accumulated resorufin fluorescence after 18 h of incubation with  
1040 HBD2 (A) and HBD3 (B) at the concentrations given. Data are expressed relative to the control and  
1041 represent means ± SD of three independent experiments conducted in triplicates. \*\*\* $p = 0.0004$  in  
1042 Two-way ANOVA. N.S: not significant ( $p = 0.7721$ ).

1044 **Figure 3**1046 **ATP quantification in *P. aeruginosa* after 18 h incubation in the presence or absence of HBD2 and HBD3 at the concentrations given.**

1047 ATP concentrations are in nM and were calculated based  
1048 on a standard curve. Shown are means ± SD of three independent experiments conducted in  
1049 duplicates.  $p = 0.01$  in One way ANOVA with Bonferroni posthoc analysis for 2 μM HBD2  
1050 compared to 2 μM HBD3.

1051 **Figure 4**

1052 **Effects of HBD2 on *A. baumannii* biofilm formation and metabolic activity.** Shown are crystal  
1053 violet absorbance and accumulated resorufin fluorescence expressed as % of the control after 18 h of  
1054 incubation with HBD2 at the concentrations given. Data represent means ± SD of three independent  
1055 experiments conducted in triplicates. \*\* $p = 0.004$  for biofilm reduction *versus* reduction of metabolic  
1056 activity in two tailed Paired Samples Test. In Oneway ANOVA with Bonferroni posthoc analysis,  $p$   
1057 =0.001 for resazurin reduction at 4 μM HBD2, and  $p < 0.001$  for biofilm reduction at 1, 2, and 4 μM  
1058 HBD2, compared to the solvent control. All other data points were not significantly different from  
1059 the control.

1060 **Figure 5**1062 **Comparative effects of D- HBD2 and linear HBD2 on *P. aeruginosa* biofilm and metabolic activity.**

1063 Shown are biofilm formation and accumulated resorufin fluorescence expressed as % of the  
1064 control after 18 h of incubation with all D- HBD2 (A) and linear HBD2 (B) at the concentrations  
1065 given. Data represent means ± SD of three independent experiments conducted in triplicates. In  
1066 Paired T test comparing biofilm reduction and reduction of metabolic activity, \*\*\* $p < 0.001$  for D-  
1067 HBD2 (A) and not significant (N.S.) for linear HBD2 (B). In Oneway ANOVA with Bonferroni  
1068 posthoc analysis, biofilm formation ( $p = 0.033$ ) but not metabolic activity ( $p = 0.473$ ) is significantly  
1069 reduced by D-HBD2. For linear HBD2, none of the data is significantly different from the solvent  
1070 control.

1071 **Figure 6**

1075 ***In silico* docking and binding energies ( $\Delta G$ ) of various QS molecules calculated for LasR and**  
1076 **HBD2.** AutoDock Vina was used to predict binding sites and potential hits for HBD2 and quorum  
1077 sensing molecules in comparison to LasR. (A) Test *N*-(3-oxohexanoyl) homoserine lactone (3-oxo-  
1078 C12-HSL, green) lies inside the LasR binding pocket in the same region as co-crystallized 3-oxo-  
1079 C12-HSL (blue) with LasR (RSCB 3IX3). (B) HBD2 does not contain a binding pocket for test 3-  
1080 oxo-C12-HSL (green). Free energy of binding ( $\Delta G$ ) for various hits were determined for  
1081 phosphorylcolamine (NEtP), 3-oxo-C12-HSL, *N*-butyryl homoserine lactone (C4-HSL), and 2-  
1082 heptyl-3-hydroxy-4-quinolone (PQS) as ligands with either LasR (C) or HBD2 (D) as rigid receptors.  
1083 Dashed lines indicate the -6 kcal/mol threshold for actively bound molecules.  
1084

#### 1085 **Figure 7**

1086 **Relative gene expression of *flgF* and *pslA* in the presence and absence of 0.25  $\mu$ M HBD2 as**  
1087 **determined by qPCR.** Gene expression of *flgF* (A) and *pslA* (B) in *P. aeruginosa* was calculated  
1088 relative to the reference gene *gapA* after incubation in the presence or absence of HBD2 for up to 12  
1089 h. Shown are means  $\pm$  SEM, n = 6. In multivariate ANOVA with Bonferroni posthoc analysis ( $*p <$   
1090  $0.05$  and  $**p < 0.01$ ), gene expression of *flgF* and *pslA* changed over time (Control:  $p < 0.01$  for *flgF*  
1091 0.5 h versus 6 h and 12h, and  $p < 0.05$  for *pslA* 2 h versus 6 h and 12 h; HBD2:  $p < 0.05$  for *flgF* 0.5  
1092 h versus 12 h) but there was no significant difference between the control and HBD2 treated  
1093 bacteria.  
1094

1095

1096

#### 1096 **Figure 8**

1097 **Outer membrane protein profile of *P. aeruginosa* after 18 h incubation in the presence and**  
1098 **absence of HBD2.** (A) Four  $\mu$ L of concentrated outer membrane preparations from HBD2 treated  
1099 (0.125 – 1  $\mu$ M) or solvent control exposed bacteria (0) were resolved by SDS Tris-Tricine PAGE and  
1100 visualized by silver stain. (Med) indicates medium only processed like bacteria-containing samples.  
1101 The band migrating between 10 and 15 kDa in all samples is consistent with the expected molecular  
1102 weight of lysozyme (14 kDa) that was added to the extraction buffer. (B) Approximate molecular  
1103 weight and intensities of bands were quantified with Image Lab software and band intensities  
1104 detected in both replicates were normalized to the intensity of the presumptive lysozyme band. Each  
1105 data point represents the average of replicates. Each line represents the protein profile for the  
1106 indicated HBD2 concentration (in  $\mu$ M).  
1107

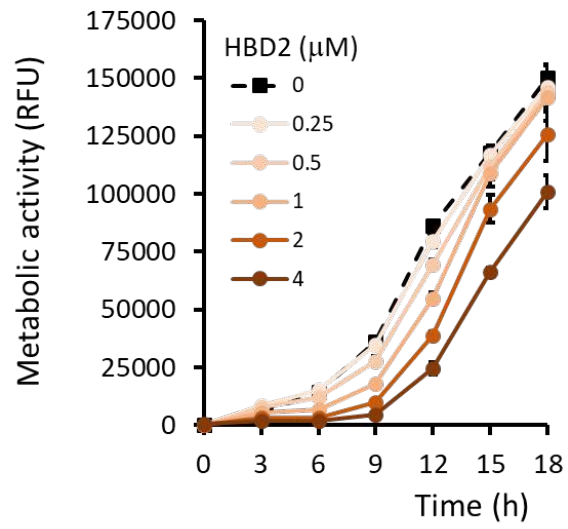
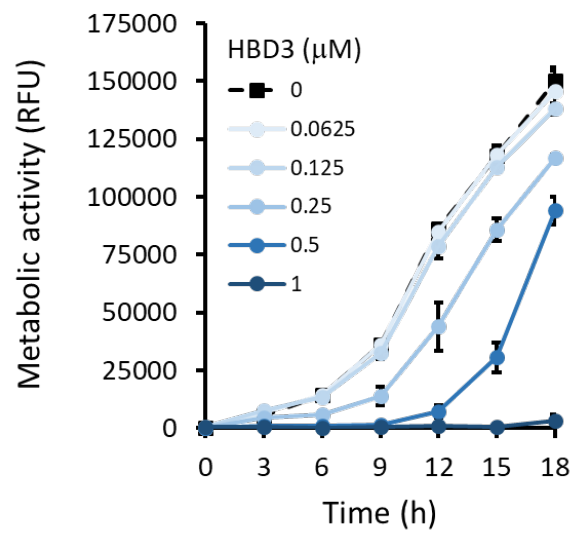
1108

1109

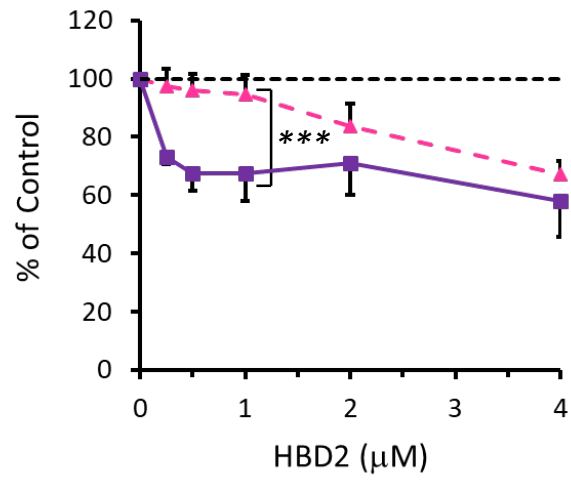
#### 1109 **Figure 9**

1110 **Atomic force microscopy of *P. aeruginosa* after 18 h incubation in the presence and absence of**  
1111 **0.25  $\mu$ M HBD2.** Bacteria were incubated on glass slides and fixed with 2.5 % glutaraldehyde prior to  
1112 imaging. Images taken with the atomic force microscope were first order flattened before extracting  
1113 measurement for bacterial roughness. (A) Representative images. CTRL: solvent control exposed  
1114 bacteria. (B) Box and whisker chart (with inner points and outliers) of roughness measurements from  
1115 multiple images of solvent exposed control bacteria (CTRL, n = 85) and 0.25  $\mu$ M HBD2 treated  
1116 bacteria (n = 69).  $*** p < 0.001$  in independent samples T test.  
1117

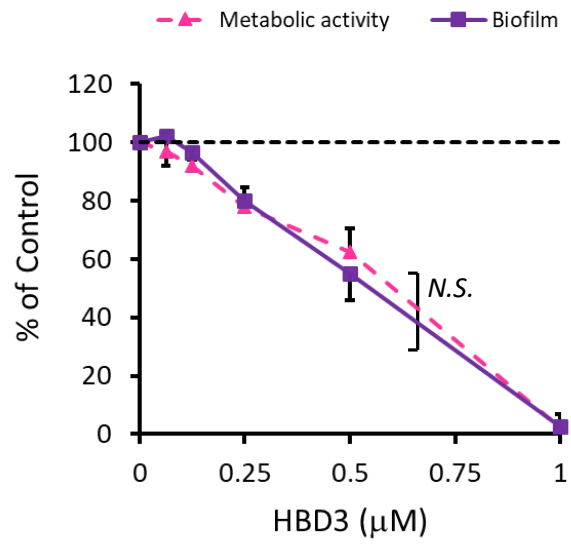
1117

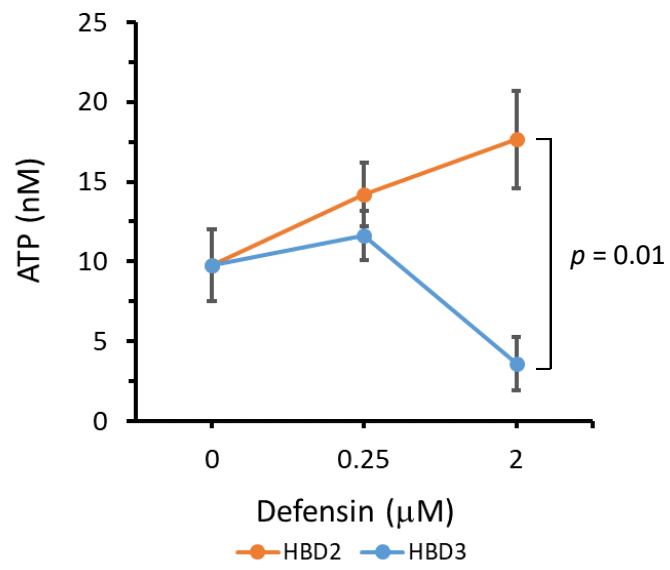
**A****B**

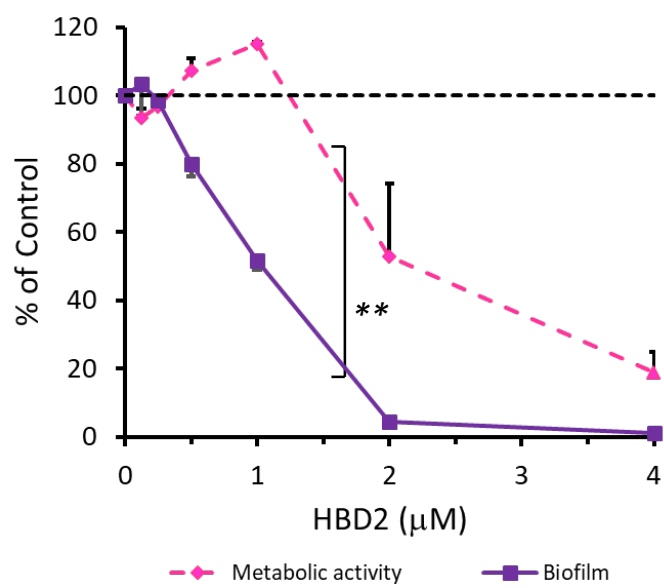
**A**



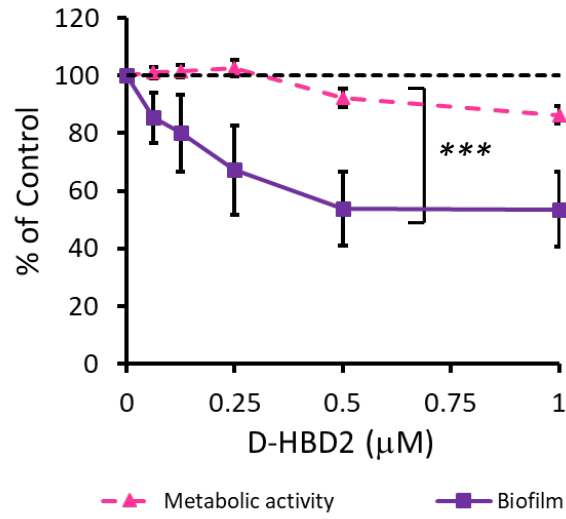
**B**



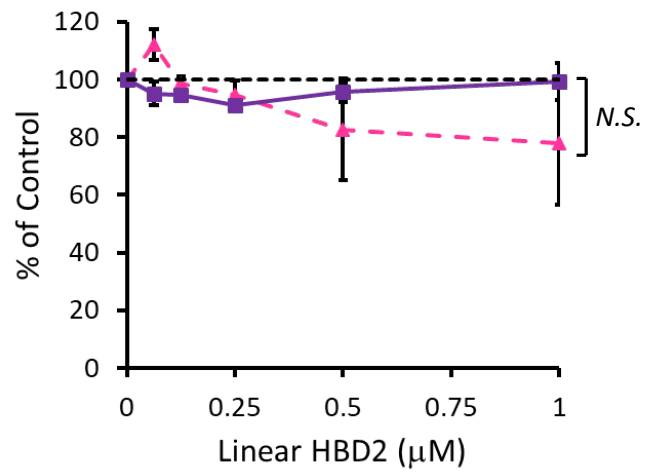




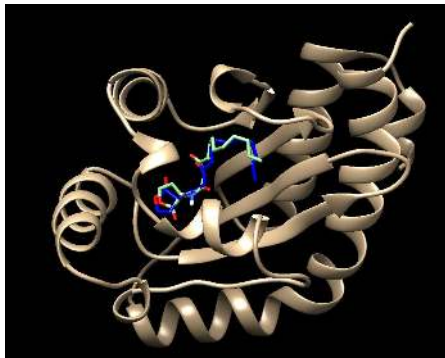
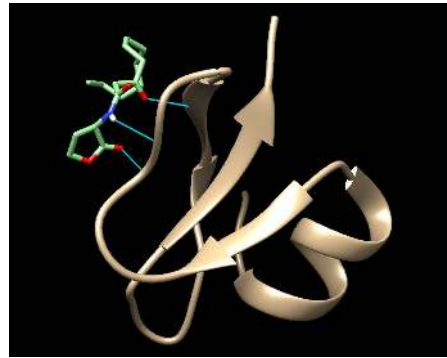
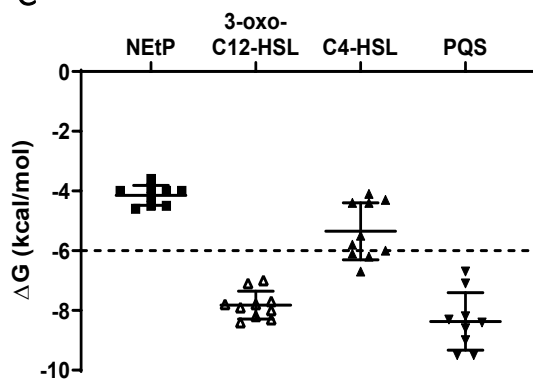
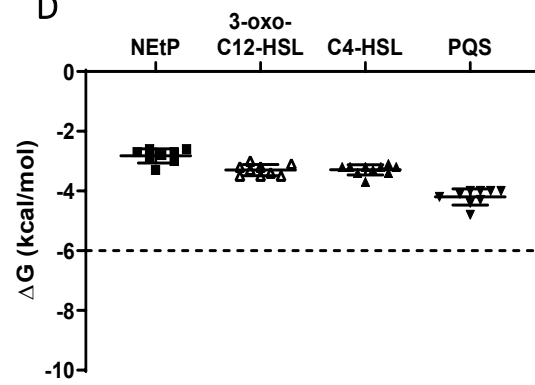
**A**



**B**

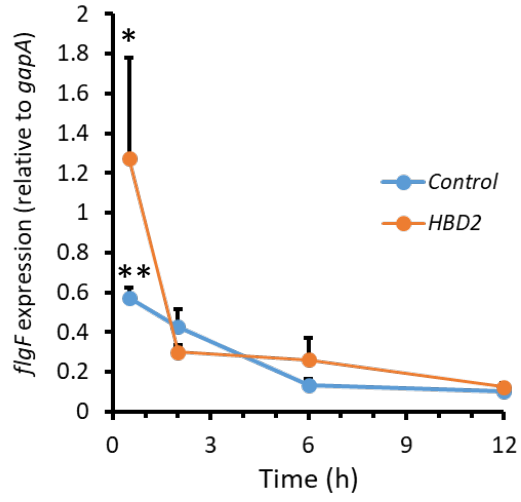




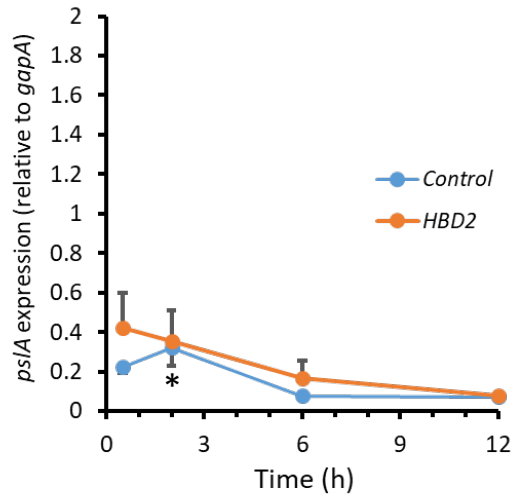
**A****LasR****B****HBD2****C****D**

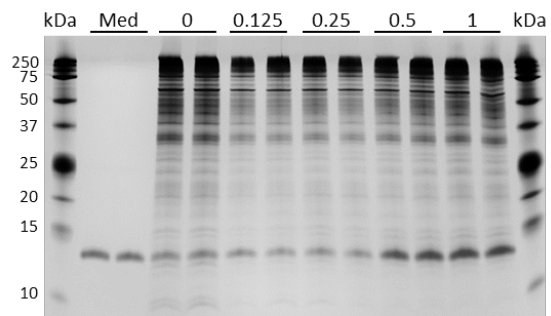
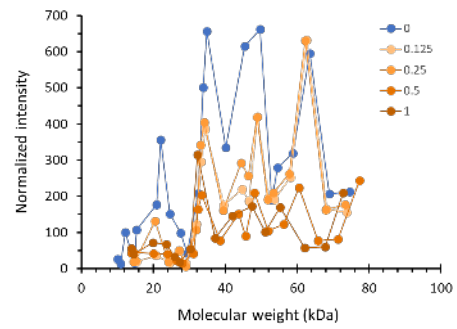


**A**

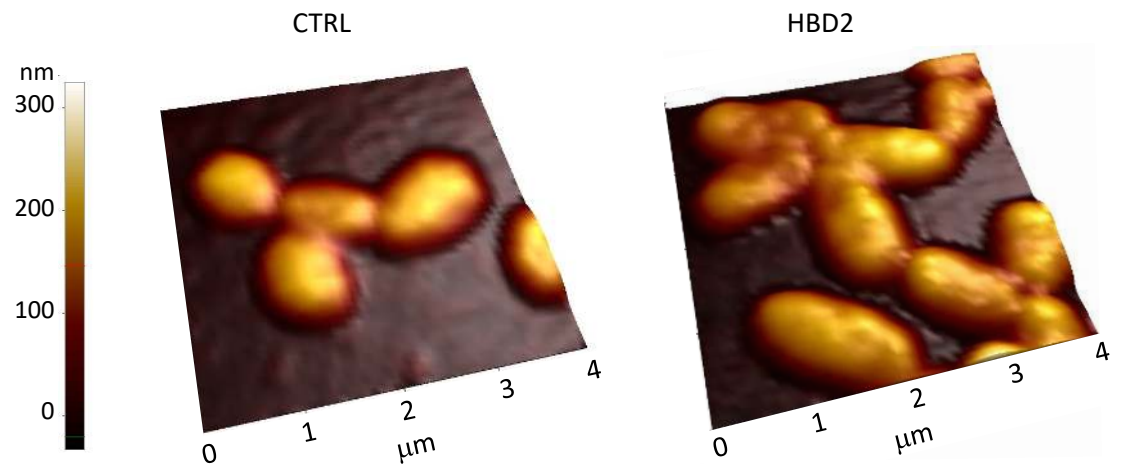


**B**



**A****B**

**A**



**B**

